

AD-781 980

**ANALYSIS OF A SINGLE-DEGREE-OF-FREEDOM
RATE-INTEGRATING GYRO**

G. H. Neugebauer

The Aerospace Corporation

Prepared for:

Air Force Systems Command

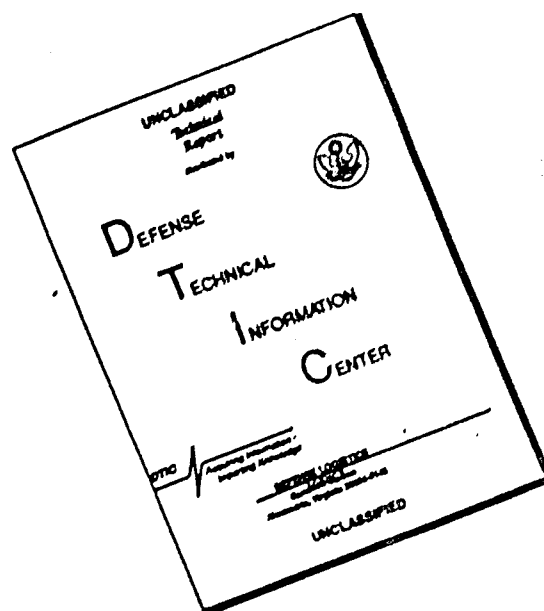
15 March 1974

DISTRIBUTED BY:

NTIS

**National Technical Information Service
U. S. DEPARTMENT OF COMMERCE
5285 Port Royal Road, Springfield Va. 22151**

DISCLAIMER NOTICE



THIS DOCUMENT IS BEST QUALITY AVAILABLE. THE COPY FURNISHED TO DTIC CONTAINED A SIGNIFICANT NUMBER OF PAGES WHICH DO NOT REPRODUCE LEGIBLY.

UNCLASSIFIED

Security Classification

AD-781980

DOCUMENT CONTROL DATA - R & D

(Security classification of title, body of abstract and indexing annotation must be entered when the overall report is classified)

1 ORIGINATING ACTIVITY (Corporate author) The Aerospace Corporation El Segundo, California		2a REPORT SECURITY CLASSIFICATION Unclassified	
		2b GROUP	
3 REPORT TITLE ANALYSIS OF A SINGLE-DEGREE-OF-FREEDOM RATE- INTEGRATING GYRO			
4 DESCRIPTIVE NOTES (Type of report and inclusive dates)			
5 AUTHOR(S) (First name, middle initial, last name) George H. Neugebauer			
6 REPORT DATE 74 MAR 15		7a TOTAL NO. OF PAGES 59	7b NO. OF REFS 0
8a CONTRACT OR GRANT NO. F04701-73-C-0074		8b ORIGINATOR'S REPORT NUMBER(S) TR-0074(4701-03)-4	
8c PROJECT NO.		8d OTHER REPORT NO(S) (Any other numbers that may be assigned this report) SAMSO-TR-74-146	
10 DISTRIBUTION STATEMENT Approved for public release; distribution unlimited			
11 SUPPLEMENTARY NOTES		12 SPONSORING MILITARY ACTIVITY Space and Missile Systems Organization Air Force Systems Command Los Angeles, California	
13 ABSTRACT The effects of asymmetry of design, manufacturing tolerances, and assembly tolerances on the dynamics of a single-degree-of-freedom, rate-integrating gyro are analyzed. The effects of many error sources and the effects of commonly accepted (but frequently erroneous) assumptions on the determination of the performance coefficients are reviewed and analyzed. Statistical analysis procedures for data reduction are not included since they are well covered in the literature. A brief investigation of convection torques due to density gradients in the flotation fluid is included. Though usually ignored, these convection torques may be very significant in some applications.			
Reprinted by NATIONAL TECHNICAL INFORMATION SERVICE U. S. Department of Commerce Springfield VA 22151			

KEY WORDS

**Gyro, Rate-Integrating
Single Degree of Freedom**

Distribution Statement (Continued)

Abstract (Continued)

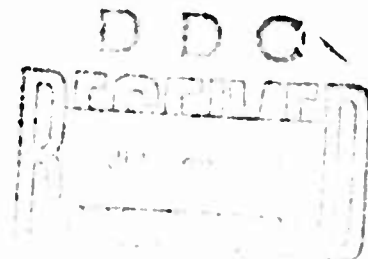
**Air Force Report No.
SAMSO-TR-74-146**

**Aerospace Report No.
TR-0074(4901-03)-4**

**ANALYSIS OF A SINGLE-DEGREE-OF-FREEDOM
RATE-INTEGRATING GYRO**

**Prepared by
G. H. Neugebauer
Control and Electromechanical Subdivision
Guidance and Control Division**

74 MAR 15



**Engineering Science Operations
THE AEROSPACE CORPORATION**

**Prepared for
SPACE AND MISSILE SYSTEMS ORGANIZATION
AIR FORCE SYSTEMS COMMAND
LOS ANGELES AIR FORCE STATION
Los Angeles, California**

Approved for public release; distribution unlimited

il

FOREWORD

This report is published by The Aerospace Corporation, El Segundo, California, under Air Force Contract F04701-73-C-0074.


This report, which documents research carried out from June 1972 through November 1973, was submitted 1 April 1974 to G. E. Aichinger, SAMSO (TM), for review and approval.

Approved



D. J. Griep, Director
Control and Electromechanical Subdivision
Guidance and Control Division
Engineering Science Operations

Publication of this report does not constitute Air Force approval of the report's findings or conclusions. It is published only for the exchange and stimulation of ideas.



Gerhard E. Aichinger
Technical Advisor
Contracts Management Office
Space and Missile Systems
Organization (TM)

CONTENTS

FOREWORD	ii
ABSTRACT	iii
1. INTRODUCTION	1
2. MISALIGNMENTS WITHIN A GYRO	3
2.1 Introduction	3
2.2 Coordinate Systems	3
2.3 Moments of Inertia	5
3. DYNAMICS OF THE GIMBAL	7
3.1 Introduction	7
3.2 Principal Axes of Rotor and Gimbal Structure	8
3.3 Angular Momentum of Rotor and Gimbal	9
3.4 Torque Equations	11
4. MODEL EQUATION	15
5. TUMBLE TESTS	
5.1 Introduction	19
5.2 Error Sources	19
5.3 Transformation of Coordinates	21
5.4 Continuous Rotation Tumble Test	23
5.5 Discrete Position Tumble Test	34
6. PRECISION LINEAR VIBRATION TEST	41
6.1 Introduction	41
6.2 Determination of D_{II} - Position No. 1	42
6.3 Determination D_{SS} - Position No. 2	44
6.4 Determination D_{IS} - Position No. 3	45
7. TORQUES DUE TO DENSITY GRADIENTS	47
APPENDIX. GLOSSARY OF SYMBOLS	53

FIGURES

2-1	Gyro Reference Axes and Gimbal Coordinate System	4
3-1.	Eccentric Applied Force	7
5-1.	Earth and Gyro Coordinate Systems.	21
5-2.	Position No. 1	24
5-3.	Position No. 2	27
6-1.	Gyro Axes in Vibration Position No. 1	42
6-2.	Gyro Axes in Vibration Position No. 2	44
7-1.	Density Distribution and Fluid Flow.	48

1. INTRODUCTION

In this report, we will derive the equations of motion for a single-degree-of-freedom, rate-integrating gyro, taking into account asymmetry of design, manufacturing tolerances, and assembly tolerances which result in non-ideal geometries and dynamics. We will also review the test methods and the data reduction procedures used in determining the performance coefficients of a gyro. Lastly, we will briefly investigate the torques due to convection currents.

There are two complementary procedures commonly used for determining the performance coefficients which we will review; they are: a) tumble tests (either continuous rotation or discrete positions) and b) precision linear vibration tests. In theory, a precision centrifuge with a counter-rotating table (not necessarily a 1:1 counter-rotation) may be used. However, in practice, the results are extremely sensitive to alignment of the counter-rotating table axis to the centrifuge axis, and therefore, that procedure will not be pursued further.

Data from tumble tests and linear vibration tests are commonly reduced by using formulae which are partially or fully computer-automated. There is seldom any thought given to the formulae used nor their applicability to a particular gyro design or its application. The simplifying assumptions (there are always such assumptions) used in the data reduction procedures may or may not be appropriate for the particular design or the application.

One of the principal purposes of this report is to review the assumptions, explicit or implicit, in the choice of test method and/or data reduction procedure. The test engineer must then review the error sources and use his judgment as to the appropriateness of the test methods and the data reduction. In some cases, analyses and/or tests may be required prior to making a final judgment.

2. MISALIGNMENTS WITHIN A GYRO

2.1 Introduction

In this section, we will investigate the effects of non-ideal geometries arising from design compromises, material variations, manufacturing tolerances, and assembly tolerances. It is usually assumed that the true spin axis (SA) as determined by the bearing geometry, is normal to the true output axis (OA) as determined by the gimbal pivot or suspension geometry. The input axis (IA) is then taken to be normal to SA and OA. Thus, the three axes form an orthogonal coordinate system. It is also generally assumed that IA, OA, and SA are principal axes of inertia for the float. In reality, none of these assumptions is likely to be exactly true.

2.2 Coordinate Systems

There are several coordinate systems that could be used in this study, each having its relative advantages and disadvantages. We will use three basic coordinate systems in our development: a) the reference system attached to the gyro case as indicated by reference markings and/or reference surfaces, b) one attached to the gyro float, and c) an inertially-fixed coordinate system. Other auxiliary coordinate systems will be used, as convenient, such as an earth-fixed coordinate system.

In any single-degree-of-freedom gyro, there are two fairly well defined axes; they are the spin axis SA and the output (pivot) axis OA. Though these axes may be well defined by geometry, they are not necessarily orthogonal, nor are they easy to locate in an assembled gyro. Assuming that the pivot clearances are very small, as is usual, then any angular motion of the gimbal relative to the gyro case must be about OA only, whether or not OA is perpendicular to SA.

The three reference axes, which are indicated by reference markings and/or reference (mounting) surfaces on the gyro case, are: a) the input reference axis (IRA), b) the output reference axis (ORA), and

c) the spin reference axis (SRA). These are nominally parallel to IA, OA, and SA, respectively, and form an orthogonal coordinate system such that the vector cross product

$$\bar{I} \times \bar{J} = \bar{K} \quad (2-1)$$

where \bar{I} , \bar{J} , and \bar{K} are unit vectors along IRA, ORA, and SRA, respectively. The origin of this coordinate system is taken to be at the centroid (C) of the gimbal (float) when at electrical null and at neutral buoyancy. For convenience, IRA, ORA, and SRA will be designated I, O, and S, respectively, as shown in Fig. 2-1.

For the gimbal, we will choose an XYZ coordinate system with the origin at C, the Y axis parallel to the true pivot axis (OA) and the YZ plane parallel to the true spin axis (SA). Let ζ_{rx} be the angle between SA' and the Z axis, as indicated in Figure 2-1, where SA' is the projection of SA on the YZ plane.

We will define the rotor as being the gyro wheel plus any associated rotating parts such as bearing races and ball retainers. The gimbal or float is defined as the complete assembly, including the rotor, that rotates as a unit about OA relative to the gyro case.

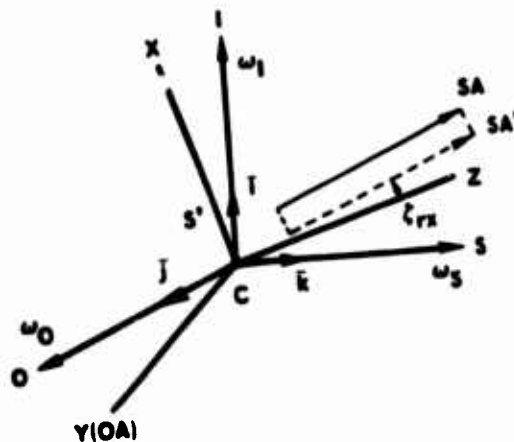


Fig. 2-1. Gyro Reference Axes and Gimbal Coordinate System

2.3 Moments of Inertia

Moments of inertia and products of inertia arise when we apply Newton's Second Law of Motion to a rotating rigid body. It is assumed that the reader is familiar with the definitions of moments of inertia and products of inertia, and we will review only those additional facts which are pertinent to our study of the gyro.

For any rigid body, with or without axes of symmetry, there are always at least three orthogonal axes passing through the centroid for which the products of inertia vanish. These axes are called principal axes and the moments of inertia about these axes are known as principal moments of inertia. Any axes of symmetry would be principal axes since the products of inertia about those axes would vanish.

The moment of inertia of the gimbal about any line p passing through the centroid may be given in terms of the principal moments of inertia J_{uu} , J_{vv} , and J_{ww} about three orthogonal principal axes U , V and W and the direction cosines, l_{pu} , l_{pv} , and l_{pw} of the line p with respect to the principal axes.

$$J_p = J_{uu} l_{pu}^2 + J_{vv} l_{pv}^2 + J_{ww} l_{pw}^2 \quad (2-2)$$

The principal moments of inertia are stationary values of Eq. (2-2), i. e., J_p is a maximum or a minimum when the line p coincides with a principal axis.

Assume that we have determined, by some means, the principal moments of inertia of the gimbal, and that the principal axes U , V , and W are nearly parallel to the I , C , and S axes, respectively, as is usually the case. Let θ_u , θ_v , and θ_w be the successive small Euler angle rotations about the U , V , and W axes, respectively, required to rotate the UVW coordinate system into the IOS coordinate system. It can be shown that the direction cosines are:

$$\begin{aligned}
l_{Iu} &\approx l_{Ov} \approx l_{Sw} \approx 1 \\
l_{Ow} &\approx -l_{Sv} \approx \theta_u \\
l_{Su} &\approx -l_{Iw} \approx \theta_v \\
l_{Iv} &\approx -l_{Ou} \approx \theta_w
\end{aligned}
\tag{2-3}$$

The three principal moments of inertia of the gimbal usually differ from one another by less than an order of magnitude and the principal axes, in general, are nearly coincident with the I, O, and S axes. If θ_u , θ_v , and θ_w are each less than 0.05 rad ($< 3^\circ$), the moments of inertia of the gimbal about the reference axes, as determined from Eqs. (2-2) and (2-3), are approximated, without significant error, by:

$$\begin{aligned}
J_I &\approx J_{uu} + J_{vv} \theta_w^2 + J_{ww} \theta_v^2 \approx J_{uu} \\
J_O &\approx J_{uu} \theta_w^2 + J_{vv} + J_{ww} \theta_u^2 \approx J_{vv} \\
J_S &\approx J_{uu} \theta_v^2 + J_{vv} \theta_u^2 + J_{ww} \approx J_{ww}
\end{aligned}
\tag{2-4}$$

The above results should not be surprising, since the principal moments of inertia are stationary values with zero slope.

3. DYNAMICS OF THE GIMBAL

3.1 Introduction

Any system of forces and torques applied to a rigid body may be replaced by a single resultant force \mathbf{F}_C acting through the centroid and a single resultant torque \mathbf{T}_C . For example, consider the single force \mathbf{F}_1 shown in Fig. 3-1(a) which is eccentric to the centroid C .

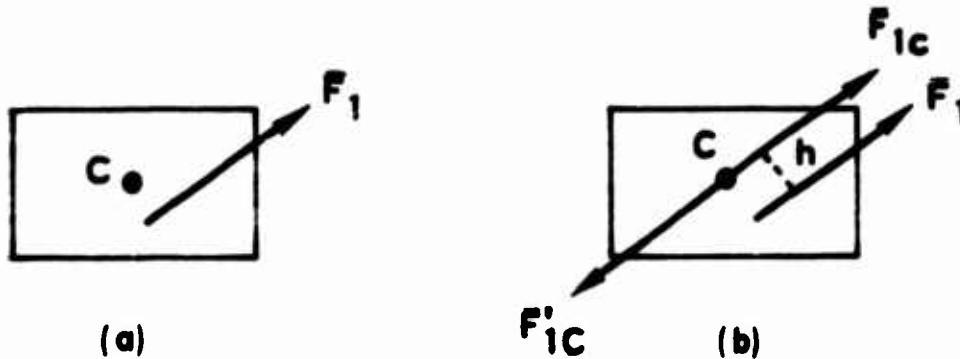


Fig. 3-1. Eccentric Applied Force

Apply two opposed forces \mathbf{F}_{1c} and \mathbf{F}'_{1c} at C in a line parallel to the line of action of \mathbf{F}_1 as shown in Fig. 3-1(b) and such that $|\mathbf{F}_{1c}| = |\mathbf{F}'_{1c}| = |\mathbf{F}_1|$. Since the vector sum of \mathbf{F}_{1c} and \mathbf{F}'_{1c} is zero, the net force acting on the body is unchanged. However, we can now consider the force system to be a force \mathbf{F}_{1c} acting through the centroid and a torque $\mathbf{F}_1 h$ due to the couple formed by the forces \mathbf{F}_1 and \mathbf{F}'_{1c} . The same procedure may be followed for each non-central force. All the resultant forces acting through the centroid may be summed vectorially to obtain but a single resultant force \mathbf{F}_C and all the torques may be summed vectorially to obtain a single resultant torque \mathbf{T}_C .

The resulting motion of the rigid body may be considered as a linear translation of the centroid due to the resultant force \mathbf{F}_C and a change in angular momentum due to the resultant torque \mathbf{T}_C . Assuming a constant mass, the differential equations of motion are:

$$\mathbf{F}_c = d(m\mathbf{\bar{V}}_c)/dt = m\mathbf{\bar{a}}_c \quad (3-1)$$

$$\mathbf{T}_c = d\mathbf{\bar{H}}/dt \quad (3-2)$$

where

m = mass

$\mathbf{\bar{V}}_c$ = velocity vector of centroid

$\mathbf{\bar{a}}_c$ = acceleration vector of centroid

$\mathbf{\bar{H}}$ = angular momentum vector

t = time

Equation (3-1) states that the rate of change of the linear momentum ($m\mathbf{\bar{V}}_c$) is equal in magnitude and direction to the resultant applied force \mathbf{F}_c acting through the centroid. Equation (3-2) states that the rate of change of the angular momentum ($\mathbf{\bar{H}}$) is equal in magnitude and direction to the resultant applied torque \mathbf{T}_c . Equation (3-2) is easily derived from the basic Eq. (3-1).

Though we are primarily interested in the angular motions of the gimbal and will stress the use of Eq. (3-2), the gimbal structure is not a perfectly rigid body and compliance torques resulting from linear acceleration of the centroid will also be considered. Of course, a gyro designer must consider the translational forces acting on the pivots, rotor bearings, and other parts for strength as well as for minimizing deflections.

3.2 Principal Axes of Rotor and Gimbal Structure

Because of tight manufacturing tolerances, accurate dynamic balancing, and extreme care in assembly, the spin axis (SA) is a principal axis of the rotor. The other principal axes of the rotor must be in a plane normal to SA and passing through the centroid of the rotor. We will assume that all axes in that plane and passing through the centroid are principal axes of inertia and, therefore, the moments of inertia about these axes are all equal. The above assumption is true for the vast

majority of gyros. There are a few gyros, such as the "Nutatron", which are purposely designed to have a rotor with unequal moments of inertia about their two radial principal axes of inertia, but such gyros are not yet commercially significant.

Manufacturing and assembly tolerances for the gimbal do not permit as accurate a knowledge of the location of the principal axes as we had for the rotor alone. However, gimbals are generally designed so that the principal axes are nominally parallel to the X, Y, and Z axes and the Y axis passes through or close to the centroid C of the gimbal. Therefore, we may use Eqs. (2-4) for the gimbal, without appreciable error, for the vast majority of gyros and we will so assume.

3.3 Angular Momentum of Rotor and Gimbal

Since the only axes externally available are the reference axes (I, O, and S in Fig. 2-1), we will determine the angular momentum of the gyro with respect to these axes. Consider first the angular momentum of the rotor relative to the gimbal.

The angular momentum components of the rotor relative to the gimbal in the XYZ coordinate system are:

$$H_{rx} = 0$$

$$H_{ry} = -J_r \omega_r \zeta_{rx} = -H_r \zeta_{rx} \quad (3-3)$$

$$H_{rz} = J_r \omega_r = H_r$$

where

$H_r = J_r \omega_r$ = angular momentum of the rotor (plus associated rotating parts) relative to the gimbal

J_r = moment of inertia of the rotor about its axis of rotation

ω_r = angular velocity of the rotor relative to the gimbal

ζ_{rx} = misalignment angle as defined in Fig. 2-1

In order to determine the angular momentum components of the rotor relative to the gimbal in the IOS system, we will perform the following transformations:

- a) Rotate the XYZ system about the Y axis through the small angle $-\varphi_O$ required to bring the gimbal back to its electrical null position,
- b) Rotate the resulting system successively through the small Euler angles ζ_x , ζ_y , and ζ_z to bring it into coincidence with the IOS system which is fixed to the gyro case.

Since the rotation angles are all small ($\ll 1$ rad), we may use small angle approximations for the sines and cosines and neglect products of the sines. We find the angular momentum of the rotor in the IOS system relative to the gimbal is:

$$\vec{H}_r \approx H_r(\varphi_O - \zeta_y) \vec{i} + H_r(\zeta_x - \zeta_{rx}) \vec{j} + H_r \vec{k} \quad (3-4)$$

Assuming the principal axes of inertia of the gimbal are nominally parallel to the I, O, and S axes, then using Eqs. (2-4), the angular momentum of the gimbal with the rotor locked in the IOS system is:

$$\vec{H}_g = J_I \omega_I \vec{i} + J_O(\omega_O + \dot{\varphi}_O) \vec{j} + J_S \omega_S \vec{k} \quad (3-5)$$

where

$\omega_I, \omega_O, \omega_S$ = angular velocity components of the gyro case relative to inertial space about the I, O, and S axes, respectively (see Fig. 2-1).

$\dot{\varphi}_O$ = angular velocity of the gimbal relative to the gyro case about OA and $\varphi_O \ll 1$.

The total angular momentum of the gimbal is the sum of Eqs. (3-4) and (3-5). As a mnemonic device, with no loss in generality, let $(\zeta_x - \zeta_{rx}) = \zeta_I$ and $\zeta_y = \zeta_O$, then the total angular momentum of the gimbal is:

$$\begin{aligned} \bar{H} = \bar{H}_r + \bar{H}_g = & [H_r(\varphi_O - \zeta_O) + J_I \omega_I] \bar{I} \\ & + [H_r \zeta_I + J_O(\omega_O + \dot{\varphi}_O)] \bar{J} + [H_r + J_S \omega_S] \bar{K} \end{aligned} \quad (3-6)$$

3.4 Torque Equations

The torque components about the I, O, and S axes required to obtain changes in angular momentum are determined by applying Eqs. (3-2) and (3-7), below, to Eq. (3-6).

$$\begin{aligned} d\bar{I}/dt &= \omega_S \bar{J} - \omega_O \bar{K} \\ d\bar{J}/dt &= \omega_I \bar{K} - \omega_S \bar{I} \\ d\bar{K}/dt &= \omega_O \bar{I} - \omega_I \bar{J} \end{aligned} \quad (3-7)$$

$$\begin{aligned} T_I \approx & H_r(\omega_O + \dot{\varphi}_O - \zeta_I \omega_S) + J_I \dot{\omega}_I + J_r \dot{\omega}_r(\varphi_O - \zeta_O) \\ & - J_O \dot{\varphi}_O \omega_S - (J_O - J_S) \omega_O \omega_S \end{aligned} \quad (3-8)$$

$$\begin{aligned} T_O \approx & -H_r [\omega_I - (\varphi_O - \zeta_O) \omega_S] + J_O(\dot{\omega}_O + \ddot{\varphi}_O) \\ & + J_r \zeta_I \dot{\omega}_r - (J_S - J_I) \omega_S \omega_I \end{aligned} \quad (3-9)$$

$$\begin{aligned} T_S \approx & -H_r [(\varphi_O - \zeta_O) \omega_O - \zeta_I \omega_I] + J_S \dot{\omega}_S + J_r \dot{\omega}_r \\ & + J_O \dot{\varphi}_O \omega_I - (J_I - J_O) \omega_I \omega_O \end{aligned} \quad (3-10)$$

It is customary, for purposes of comparison, to normalize the torque components by dividing them by the angular momentum H_r of the rotor relative to the gimbal. It is also common practice to break out the normalized viscous drag torque $(-C\dot{\varphi}_O/H_r)$ which opposes the angular

velocity $\dot{\varphi}_O$, the normalized elastic restraint torque $(-K_e \varphi_O/H_r)$ which opposes the angular displacement φ_O , and lastly, the normalized command torque $(-K_T i)$ where:

C = damping coefficient

K_e = elastic restraint coefficient

K_T = torquer scale factor

i = torquing current

The sign convention adopted for the torquing current is such that a positive current will exert a negative torque about OA or, equivalently, will cause a positive precession rate about IA when the gimbal is maintained at its null position. The normalized torques about the I, O, and S axes are:

$$\begin{aligned} \frac{T_I}{H_r} = M_I = & (\omega_O + \dot{\varphi}_O - \zeta_I \omega_S) + \frac{J_I}{H_r} \dot{\omega}_I + \frac{\dot{\omega}_r}{\omega_r} (\varphi_O - \zeta_O) \\ & - \frac{J_O}{H_r} \dot{\varphi}_O \omega_S - \frac{J_O - J_S}{H_r} \omega_O \omega_S \end{aligned} \quad (3-11)$$

$$\begin{aligned} \frac{T_O}{H_r} = M_O = & -\frac{C}{H_r} \dot{\varphi}_O - \frac{K_e}{H_r} \varphi_O - K_T i = -[\omega_I - (\varphi_O - \zeta_O) \omega_S] \\ & + \frac{J_O}{H_r} (\dot{\omega}_O + \ddot{\varphi}_O) + \zeta_I \frac{\dot{\omega}_r}{\omega_r} - \frac{J_S - J_I}{H_r} \omega_S \omega_I \end{aligned} \quad (3-12)$$

$$\begin{aligned} \frac{T_S}{H_r} = M_S = & -[(\varphi_O - \zeta_O) \omega_O - \zeta_I \omega_I] + \frac{J_S}{H_r} \dot{\omega}_S + \frac{\dot{\omega}_r}{\omega_r} \\ & + \frac{J_O}{H_r} \dot{\varphi}_O \omega_I - \frac{J_I - J_O}{H_r} \omega_I \omega_O \end{aligned} \quad (3-13)$$

where M_I and M_S are the total applied normalized torque components about the I and S axes, respectively, and M_O is the total normalized torque about

the O axis plus the normalized viscous drag torque, the normalized elastic restraint torque, and the normalized command torque, i.e.,

$$M_O = \frac{T_O}{H_r} + \frac{C}{H_r} \dot{\varphi}_O + \frac{K_e}{H_r} \varphi_O + K_T i \quad (3-14)$$

If the misalignment angles ζ_I and ζ_O are negligible and if the gimbal is maintained at its null position ($\varphi_O = 0$), then Eqs. (3-11), (3-12), (3-13) become the following well-known equations:

$$\begin{aligned} M_I &= \omega_O + \frac{J_I}{H_r} \dot{\omega}_I - \frac{J_O - J_S}{H_r} \omega_O \omega_S \\ M_O - K_T i &= -\omega_I + \frac{J_O}{H_r} \dot{\omega}_O - \frac{J_S - J_I}{H_r} \omega_S \omega_I \\ M_S &= \frac{J_S}{H_r} \dot{\omega}_S + \frac{\dot{\omega}_r}{\omega_r} - \frac{J_I - J_O}{H_r} \omega_I \omega_O \end{aligned} \quad (3-15)$$

Note that if $\omega_O = \omega_S = i = 0$, then from the second of Eqs. (3-15), we see that a positive applied normalized moment M_O will result in a negative precession rate when the gimbal is maintained at its null position.

4. MODEL EQUATION

In most applications and tests, the gimbal is maintained at or close to its electrical null position by a platform or table slaved to the gyro and/or by a feedback torquing current. The null error will depend on the tightness of the servo loop. We may rewrite Eq. (3-12) with $\dot{\varphi}_O = \varphi_O = 0$ and M_O expressed in black box form as a function of acceleration. Variables other than acceleration, such as power supply variations and temperature variations, are not usually included in the model equation, but are treated as random variables which result in uncertainties in the drift rates. Unfortunately, there are several model equations in common use. Some are expressed in terms of drift rates, others are expressed in terms of normalized torques which have the dimensions of drift rates but are of opposite sign. Some equations are expressed in terms of acceleration inputs, whereas others are expressed in terms of specific force inputs which have opposite signs. Therefore, it is hardly surprising that there is some confusion, and that some model equations are incorrect.

Up to this point, we have not specified any dimensional units in the various equations, but merely expected them to be consistent. For example, Eqs. (3-11), (3-12), and (3-13) would be dimensionally consistent if the applied torques are in dyne-cm, the angular momentum in $\text{gm} \cdot \text{cm}^2/\text{s}$, the moments of inertia in $\text{gm} \cdot \text{cm}^2$, the angles in radians, the angular rates in rad/s , and the angular accelerations in rad/s^2 . In our model equation, we will adopt the more common practice of expressing ω_I , ω_O , and ω_S in deg/hr and $\dot{\omega}_O$ in $(\text{deg/hr})/\text{s}$. We will leave ω_r and $\dot{\omega}_r$ in rad/s and rad/s^2 . We will also adopt the practice of expressing the acceleration in units of the local g value. The model equation and the definition of symbols follow.

$$\begin{aligned} \omega_I = & D_F + D_I a_I + D_O a_O + D_S a_S + D_{II} a_I^2 + D_{OO} a_O^2 + D_{SS} a_S^2 \\ & + D_{IO} a_I a_O + D_{OS} a_O a_S + D_{IS} a_I a_S + K_T i - \zeta_O \omega_S \\ & + \frac{J_O}{H_r} \dot{\omega}_O + 206,300 \zeta_I \frac{\dot{\omega}_r}{\omega_r} - \frac{(J_S - J_I)}{H_r} \frac{\omega_S \omega_I}{206,300} \end{aligned} \quad (4-1)$$

Note that the $1 \text{ deg/hr} = 1 \text{ } \widehat{\text{sec}}/\text{s}$ and $1 \text{ rad/s} \approx 206,300 \text{ } \widehat{\text{sec}}/\text{s}$.

$\omega_I, \omega_O, \omega_S$	= angular rate components of the gyro case about the reference axes with respect to inertial space - deg/hr
$\dot{\omega}_O$	= angular acceleration of the gyro case about ORA - (deg/hr)/s
a_I, a_O, a_S	= components of total applied acceleration, \bar{a} , along the reference axes - \underline{g}
$\bar{a} = \bar{a}_T - \underline{g}$	= applied acceleration vector - \underline{g}
\bar{a}_T	= total acceleration vector with respect to inertial space - \underline{g}
\underline{g}	= gravity vector (in direction of maximum gravity gradient) - \underline{g}
\underline{g}	= unit of acceleration equal in magnitude to the local (or standard) gravity value
D_F	= fixed restraint (bias) drift rate - deg/hr
D_I, D_O, D_S	= linear, acceleration-sensitive drift rate coefficients - (deg/hr)/ \underline{g}
D_{II}, D_{OO}, D_{SS}	= quadratic, acceleration-sensitive drift rate coefficient - (deg/hr)/ \underline{g}^2
D_{IO}, D_{OS}, D_{IS}	= cross-coupled, acceleration-sensitive drift rate coefficients - (deg/hr)/ \underline{g}^2
K_T	= command rate scale factor (deg/hr)/A
i	= command rate current - A
J_I, J_O, J_S	= moments of inertia of the gimbal about the reference axes - gm · cm ²
ω_r	= angular rate of the rotor relative to the gimbal - rad/s
$\dot{\omega}_r$	= angular acceleration of the rotor relative to the gimbal - rad/s ²
H_r	= angular momentum of the rotor relative to the gimbal - gm · cm ² /s

ζ_I, ζ_O = misalignment of SA with respect to SRA about IRA and ORA, respectively - rad

Not all terms are necessarily required; the ones chosen depend on the gyro design and on the application. For example, some gyro engineers drop the D_{OO} term since no satisfactory physical explanation for it has been presented, nor is there incontrovertible evidence that it exists. However, the term has been included for completeness.

In most gyro tests, and in strapdown applications, the command rate-to-balance current is measured and/or recorded. It is usually assumed that $\dot{\omega}_r = 0$, particularly for those gyros with synchronous motors. This assumption may not always be valid. A common imperfection occurring in gyros is wheel hunting, which results from an interaction of the rotor inertia with the magnetic stiffness of the motor. The combination acts as a lightly-damped torsional pendulum, resulting in oscillation of the rotor angular rate about the synchronous value. The effect is started by wheel disturbances and may or may not persist with time. Solving Eq. (4-1) for the command rate-to-balance, with $\dot{\omega}_r = 0$, we have:

$$\begin{aligned}
 K_T i = & -(D_F + D_I a_I + D_O a_O + D_S a_S + D_{II} a_I^2 + D_{OO} a_O^2 + D_{SS} a_S^2 \\
 & + D_{IO} a_I a_O + D_{OS} a_O a_S + D_{IS} a_I a_S) + \omega_I + \zeta_O \omega_S - \frac{J_O}{H_r} \dot{\omega}_O \\
 & + \frac{(J_S - J_I) \omega_S \omega_I}{H_r 206,800}
 \end{aligned} \tag{4-2}$$

Eq. (4-2) will be assumed in all test data reduction for obtaining the performance coefficients D_F , etc.

5. TUMBLE TESTS

5.1 Introduction

In the usual tumble tests, the gyro is mounted on a turntable whose axis of rotation is nominally parallel to the earth's polar axis. As the turntable is rotated about its axis, the earth's gravity field is rotated relative to the gyro and many or all of the gyro coefficients are exercised. The command rate-to-balance current is measured at a series of table angles and recorded. From the data thus obtained and auxiliary information, the gyro coefficients are determined.

Tumble runs are performed by either of two basic methods:

- a) Discrete rotation runs in which the table is rotated to a series of table angles and the average command rate-to-balance current is measured at each table angle after equilibrium is attained.
- b) The table is rotated at a slow uniform rate (usually $\leq 20 \times$ earth's rate) and the command rate-to-balance current is recorded continuously. In either method, the average command rate-to-balance current is determined at a number of equally-spaced table angles and the gyro coefficients are determined by the method of least squares.

5.2 Error Sources

There are many error sources in a tumble test, both static and dynamic. Among the most important are the following:

- a) misalignment of the table axis with respect to the earth's polar axis,
- b) misalignment of the gyro reference axes with respect to the table axis and its zero reference position,
- c) non-orthogonality of the gyro output axis and the spin axis,
- d) convection torques due to density gradients (may be caused by temperature gradients or by non-homogeneous fluid),
- e) table axis of rotation changes with direction of rotation,

- f) wobble of table axis,
- g) torque signal lags due to uncompensated filters in the torquer loop and/or torque recorders
- h) motion of the gimbal relative to the gyro case due to off-neutral buoyancy temperature or unbalances,
- i) magnetic fields,
- j) motion about non-principal axes of the gimbal,
- k) bubbles, lint, or other contaminants in the fluid,
- l) power supply variations,
- m) pier motion
- n) noisy bearings,
- o) pivot friction torque due to off-neutral buoyancy temperature coupled with acceleration.

We will investigate, in some detail, error sources a), b), c) and d). Error sources e) and f) can be measured, and either corrected or the data compensated, though either may be difficult to accomplish. Sources g) and h) are dynamic type errors whose magnitude and phase are functions of table rate. Stray magnetic fields around the table should be eliminated, as far as practical, and the gyro protected by a continuous magnetic shield in order to control error source i). Error source j) may be minimized by careful gyro design and by reasonable care in alignment, as will be shown.

The last five error sources k) - o) generally cause discontinuous and/or erratic command rate-to-balance traces. Usually, they are random in nature and result in run-to-run variations which are frequently difficult to diagnose. Bubbles or lint in the fluid may, under some circumstances, appear to be a large, repeatable unbalance, or, under some circumstances, they may act like elastic restraints, or they

may cause dramatic shifts in the command rate-to-balance measurements. Pier tilts may be eliminated by automatic or manual leveling or the tilt may be monitored and the data corrected (which may be difficult).

5.3 Transformation of Coordinates

Let us derive the general transformation equations required to go from inputs in an earth-fixed coordinate system to a gyro-case-fixed coordinate system, including any additional inputs of the table relative to the earth. In Fig. 5-1, let xyz be the earth-fixed coordinate system and let uvw be the coordinate system fixed to the gyro case. Let TA be the table axis, which is nominally coincident with the z axis, with the table angle θ measured from the xz plane.

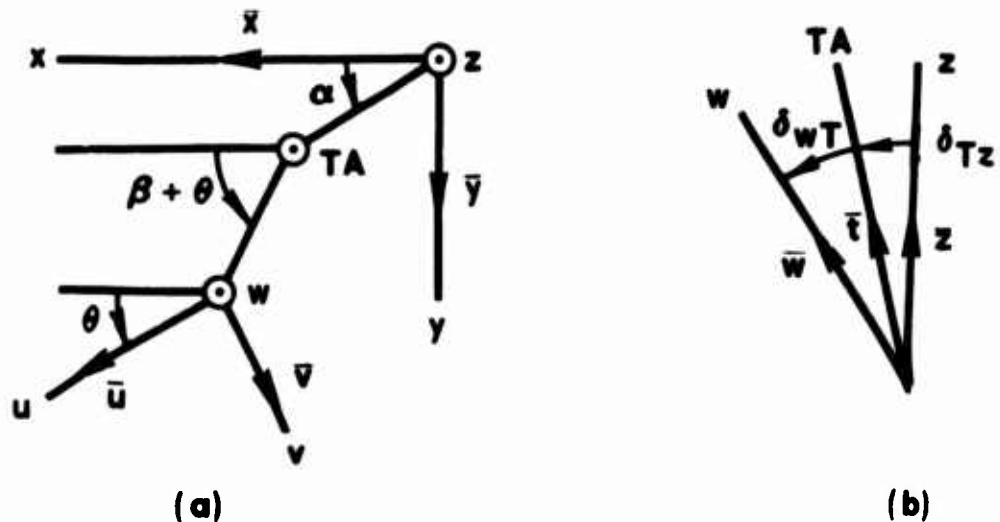


Fig. 5-1. Earth and Gyro Coordinate Systems

The table axis is slightly misaligned with the z axis, as defined by the angles δ_{Tz} and α . The w axis of the gyro is slightly misaligned with respect to TA , as defined by the angles δ_{wT} and β . Fig. 5-1(a) is a view looking in the minus z direction and Fig. 5-1(b) is a view

normal to the plane defined by TA and z axes with the w axis rotated about TA so that it is in the plane of TA and z. The angles δ_{Tz} and δ_{wT} are each $\ll 1$ radian. The angles α and β may have any values from 0 to 2π . Physically, the actual table axis may be skewed to the z axis, then TA in Fig. (5-1) is taken to be the projection of the table axis on a plane containing the z axis and parallel to the actual table axis. Similarly, the w axis shown in Fig. (5-1) is the projection of the actual w axis on a plane containing TA and parallel to the actual w axis.

Let \bar{x} , \bar{y} , \bar{z} be the vector components of earth rate ω^e of acceleration along the x, y and z axes, respectively. Let \bar{t} be the vector representing the table rate relative to earth. Let \bar{u} , \bar{v} , and \bar{w} be the total resultant vector components along the u, v, and w axes, respectively. The vector components in the uvw coordinate system, due to the inputs \bar{x} , \bar{y} , \bar{z} and \bar{t} , are determined by the following transformations:

- a) Rotate the xyz system about the z axis through the angle α to form the $x_1 y_1 z_1$ system.
- b) Rotate the $x_1 y_1 z_1$ system about the y_1 axis through the angle δ_{Tz} to form the $x_2 y_2 z_2$ system. The z_2 axis now coincides with TA, and the vector \bar{t} is now introduced.
- c) Rotate the $x_2 y_2 z_2$ system about the z_2 axis through the angle $(\beta - \alpha + \theta)$ to form the $x_3 y_3 z_3$ system.
- d) Rotate the $x_3 y_3 z_3$ system about the y_3 axis through the angle δ_{wT} to form the $x_4 y_4 z_4$ system. The z_4 axis now coincides with the w axis.
- e) Lastly, rotate the $x_4 y_4 z_4$ system about the z_4 axis through the angle $-\beta$ to coincide with the u v w system.

Since δ_{Tz} and δ_{wT} are $\ll 1$ radian, we may use small angle approximations for the trigonometric functions, i.e.,

$$\begin{aligned}\cos \delta_{Tz} &\approx \cos \delta_{wT} \approx 1 \\ \sin \delta_{Tz} &\approx \delta_{Tz} \text{ and } \sin \delta_{wT} \approx \delta_{wT} \\ \delta_{Tz} \cdot \delta_{wT} &\approx 0\end{aligned}\tag{5-1}$$

After performing the above transformations and applying the approximations of Eqs. (5-1), we find

$$\begin{aligned}
 \bar{u} &\approx \bar{x} \cos \theta + \bar{y} \sin \theta - \bar{z} [\delta_{Tz} \cos(\theta - \alpha) + \delta_{wT} \cos \beta] \\
 &\quad - \bar{t} \delta_{wT} \cos \beta \\
 \bar{v} &\approx -\bar{x} \sin \theta + \bar{y} \cos \theta + \bar{z} [\delta_{Tz} \sin(\theta - \alpha) - \delta_{wT} \sin \beta] \\
 &\quad - \bar{t} \delta_{wT} \sin \beta \\
 \bar{w} &\approx \bar{x} [\delta_{Tz} \cos \alpha + \delta_{wT} \cos(\beta + \theta)] + \bar{y} [\delta_{Tz} \sin \alpha \\
 &\quad + \delta_{wT} \sin(\beta + \theta)] + \bar{z} + \bar{t}
 \end{aligned} \tag{5-2}$$

5.4 Continuous Rotation Tumble Test

We will first consider the tumble test in which the table is rotated continuously and uniformly with respect to earth. The discrete position tumble test will be investigated in a later section.

5.4.1 Position No. 1, ORA \rightarrow North

With the table axis nominally parallel to the earth's polar axis EA, mount the gyro on the table so that ORA is nominally parallel to TA and points north, and IRA points west when the table angle $\theta = 0^\circ$. Fig. 5-2 shows the relative directions of the various axes. Fig. 5-2(a) is a view looking south along EA and Fig. 5-2(b) is a view normal to the plane of EA and TA with ORA rotated about TA into the plane of EA and TA. The misalignment angles δ_{TE} and δ_{ONT} correspond to δ_{Tz} and δ_{wT} of Fig. 5-1 and are greatly exaggerated.

The table will be rotated at a rate $b\omega_E$, relative to earth, in a counterclockwise direction (same direction as earth rate) and then in a clockwise direction, i. e., $-b\omega_E$ relative to earth.

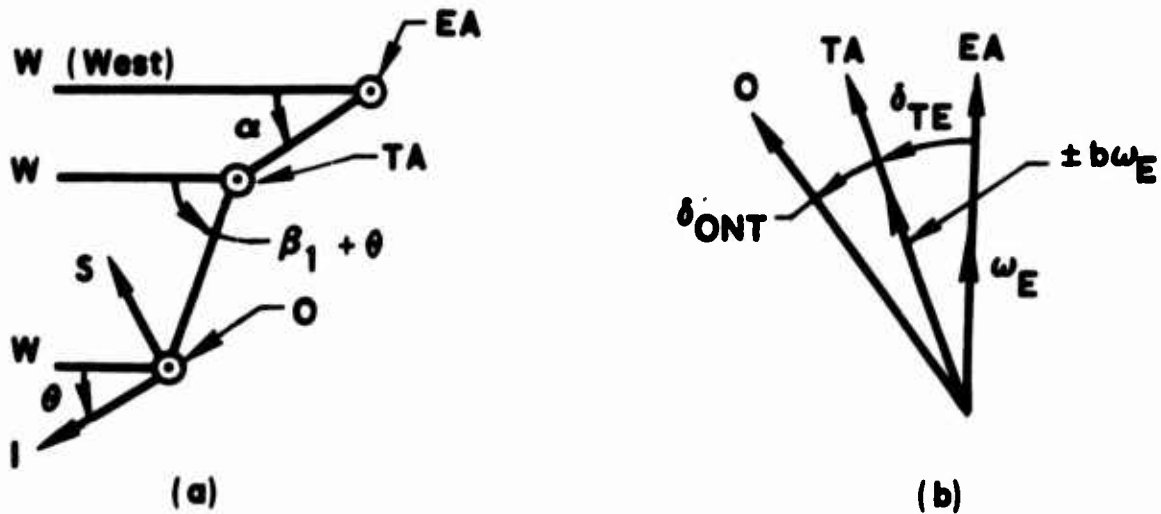


Fig. 5-2. Position No. 1

5.4.1.1 Counterclockwise Rotation of the Table: The angular velocity components to be substituted in Eqs. (5-2) are $\bar{x} = 0$, $\bar{y} = 0$, $\bar{z} = \omega_E$, and $\bar{t} = b\omega_E$. The angular velocity vectors ω_I , ω_O , and ω_S correspond to the vectors \bar{u} , \bar{w} , and $-\bar{v}$ of Eqs. (5-2), respectively.

$$\begin{aligned}\omega_I &\approx -\omega_E [(1+b) \delta_{ONT} \cos \beta_1 + \delta_{TE} \cos(\theta - \alpha)] \\ \omega_O &\approx \omega_E (1+b) \\ \omega_S &\approx \omega_E [(1+b) \delta_{ONT} \sin \beta_1 - \delta_{TE} \sin(\theta - \alpha)] \\ \dot{\omega}_O &\approx 0\end{aligned}\tag{5-3}$$

The acceleration components to be substituted in Eq. (5-2) are $\bar{x} = \bar{t} = 0$, $\bar{y} = \cos \lambda$, $\bar{z} = \sin \lambda$, where λ is the astronomic latitude (positive in northern hemisphere). The acceleration components a_I , a_O , a_S correspond to the vectors \bar{u} , \bar{w} , and $-\bar{v}$, respectively of Eqs. (5-3).

$$\begin{aligned}a_I &\approx \cos \lambda \sin \theta - \sin \lambda [\delta_{ONT} \cos \beta_1 + \delta_{TE} \cos(\theta - \alpha)] \\ a_O &\approx \sin \lambda + \cos \lambda [\delta_{ONT} \sin(\beta_1 + \theta) + \delta_{TE} \sin \alpha] \\ a_S &\approx -\cos \lambda \cos \theta + \sin \lambda [\delta_{ONT} \sin \beta_1 - \delta_{TE} \sin(\theta - \alpha)]\end{aligned}$$

At middle latitudes (25° to 60°) where practically all gyro testing is performed, the effects of small misalignments on the acceleration components will result in only second-order errors in the drift rates and will be neglected.

$$a_I \approx \cos \lambda \sin \theta$$

$$a_O \approx \sin \lambda \quad (5-4)$$

$$a_S \approx -\cos \lambda \cos \theta$$

Substitute Eqs. (5-3) and (5-4) in Eq. (4-2). Let i_{ONk} be the command rate-to-balance current in Position No. 1 (ORA \rightarrow North) with counterclockwise rotation at table angle $\theta_k = k\theta_n$, where $\theta_n = 360^\circ/n$ and $k = 1, 2, 3, \dots, n$. The terms are arranged as in a Fourier series.

$$\begin{aligned} K_T i_{ONk} = & - [D_F + D_O \sin \lambda + D_{OO} \sin^2 \lambda + 1/2(D_{II} + D_{SS}) \cos^2 \lambda \\ & + \omega_E (1+b) \delta_{ONT} (\cos \beta_1 - \zeta_O \sin \beta_1) \\ & + \frac{J_S - J_I}{412,600 H_r} \omega_E^2 (1+b)^2 \delta_{ONT}^2 \sin 2\beta_1] \\ & - [D_I \cos \lambda + 1/2 D_{IO} \sin 2\lambda + \omega_E \delta_{TE} (\sin \alpha + \zeta_O \cos \alpha) \\ & - \frac{J_S - J_I}{206,300 H_r} \omega_E^2 (1+b) \delta_{ONT} \delta_{TE} \cos(\alpha + \beta_1)] \sin k\theta_n \\ & + 1/2 [D_{IS} \cos^2 \lambda + \frac{J_S - J_I}{206,300 H_r} \omega_E^2 \delta_{TE}^2 \cos 2\alpha] \sin 2k\theta_n \\ & + [D_S \cos \lambda + 1/2 D_{OS} \sin 2\lambda - \omega_E \delta_{TE} (\cos \alpha - \zeta_O \sin \alpha) \\ & - \frac{J_S - J_I}{206,300 H_r} \omega_E^2 (1+b) \delta_{ONT} \delta_{TE} \sin(\alpha + \beta_1)] \cos k\theta_n \\ & + 1/2 [(D_{II} - D_{SS}) \cos^2 \lambda - \frac{J_S - J_I}{206,300 H_r} \omega_E^2 \delta_{TE}^2 \sin 2\alpha] \cos 2k\theta_n \end{aligned} \quad (5-5)$$

5.4.1.2 Clockwise Rotation of the Table: The setup is the same as in Fig. 5-2, but the table is now rotated in the opposite direction without disturbing the setup used for the counterclockwise rotation. The command rate-to-balance equation is the same as Eq. (5-5), except that $(1+b)$ is replaced by $(1-b)$, and the command rate-to-balance current is i'_{ONk} at table angle $\theta_k = k\theta_n$. Though the table is rotating clockwise, the table angle θ_k is still measured in a counterclockwise direction from the west, as shown in Fig. 5-2(a).

5.4.1.3 Weighting the Data from Position No. 1: In order to eliminate some of the effects of the gyro misalignment angle δ_{ONT} and to minimize the remaining effects, we will weight the data as follows:

$$\begin{aligned}
 W_{ONk} = \frac{K_T}{2b} [(b-1) i_{ONk} + (b+1) i'_{ONk}] = & -[D_F + D_O \sin \lambda \\
 & + D_{OO} \sin^2 \lambda + 1/2(D_{II} + D_{SS}) \cos^2 \lambda \\
 & + \frac{J_S - J_I}{412,600 H_F} \omega_E^2 (b^2 - 1) \delta_{ONT}^2 \sin 2\theta_1] - [D_I \cos \lambda \\
 & + 1/2 D_{IO} \sin 2\lambda + \omega_E \delta_{TE} (\sin \alpha + \zeta_O \cos \alpha)] \sin k\theta_n \\
 & + 1/2 [D_{IS} \cos^2 \lambda + \frac{J_S - J_I}{206,300 H_F} \omega_E^2 \delta_{TE}^2 \cos 2\alpha] \sin 2k\theta_n \\
 & + [D_S \cos \lambda + 1/2 D_{OS} \sin 2\lambda - \omega_E \delta_{TE} (\cos \alpha \\
 & - \zeta_O \sin \alpha)] \cos k\theta_n + 1/2 [(D_{II} - D_{SS}) \cos^2 \lambda \\
 & - \frac{J_S - J_I}{206,300 H_F} \omega_E^2 \delta_{TE}^2 \sin 2\alpha] \cos 2k\theta_n \quad (5-6)
 \end{aligned}$$

5.4.2 Position No. 2, ORA → South

Position No. 2 is obtained from Position No. 1 by rotating the gyro 180° about SRA so that ORA points south along TA and IRA points east

when $\theta = 0^\circ$. Rotating about SRA minimizes the time required for settling. In the following analysis, it is assumed that the position of TA relative to EA is unchanged. If this is not true in any particular test setup, then the analysis must be appropriately modified and becomes more complicated. However, in general, the angle that ORA makes with TA would not be the same as in Position No. 1.

Fig. 5-3 shows the relative directions of the axes. Fig. 5-3(a) is a view looking south along EA, and Fig. 5-3(b) is a view normal to the plane of EA and TA with ORA rotated about TA into the plane of EA and TA.

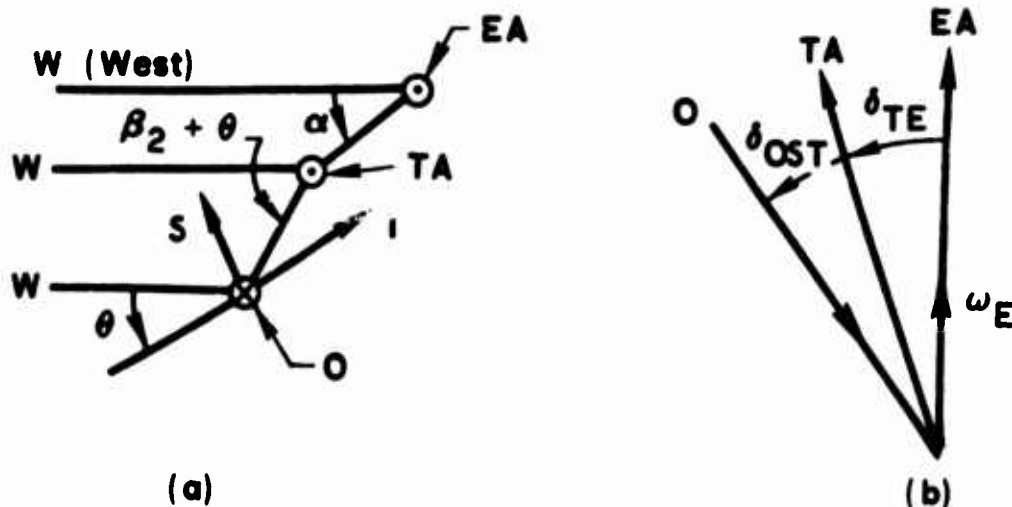


Fig. 5-3. Position No. 2

5.4.2.1 Counterclockwise Rotation of the Table: Let the table rotate counterclockwise ($\dot{\theta} > 0$) at a constant rate $b\omega_E$ with respect to earth. The angular velocity vectors to be substituted in Eqs. (5-2) are $\bar{x} = \bar{y} = 0$, $\bar{z} = \omega_E$, and $\bar{t} = b\omega_E$. The angular velocity components ω_I , ω_O , and ω_S correspond to $-\bar{u}$, $-\bar{w}$, and $-\bar{v}$, respectively of Eqs. (5-2).

$$\begin{aligned}
\omega_I &\approx -\omega_E [(1+b) \delta_{OST} \cos \beta_2 - \delta_{TE} \cos(\theta - \alpha)] \\
\omega_O &\approx -\omega_E (1+b) \\
\omega_S &\approx \omega_E [(1+b) \delta_{OST} \sin \beta_2 - \delta_{TE} \sin(\theta - \alpha)] \\
\dot{\omega}_O &\approx 0
\end{aligned} \tag{5-7}$$

The equivalent applied acceleration components along the gyro reference axes are also determined from Eqs. (5-2) and simplified.

$$\begin{aligned}
a_I &\approx -\cos \lambda \sin \theta \\
a_O &\approx -\sin \lambda \\
a_S &\approx -\cos \lambda \cos \theta
\end{aligned} \tag{5-8}$$

Substitute Eqs. (5-7) and (5-8) in Eq. (4-2). Let i_{OSk} be the command rate-to-balance current in Position No. 2 (ORA \rightarrow South) with counterclockwise rotation at table angle $\theta_k = k\theta_n$, where $k = 1, 2, 3, \dots, n$.

$$\begin{aligned}
K_T i_{OSk} = & -[D_F - D_O \sin \lambda + D_{OO} \sin^2 \lambda + 1/2(D_{II} + D_{SS}) \cos^2 \lambda \\
& + \omega_E (1+b) \delta_{OST} (\cos \beta_2 - \zeta_O \sin \beta_2) \\
& + \frac{J_S - J_I}{412,600 H_F} \omega_E^2 (1+b)^2 \delta_{OST}^2 \sin 2\beta_2] \\
& + [D_I \cos \lambda - 1/2 D_{IO} \sin 2\lambda + \omega_E \delta_{TE} (\sin \alpha - \zeta_O \cos \alpha) \\
& + \frac{J_S - J_I}{206,300 H_F} \omega_E^2 (1+b) \delta_{OST} \delta_{TE} \cos(\alpha + \beta_2)] \sin k\theta_n \\
& - 1/2 [D_{IS} \cos^2 \lambda + \frac{J_S - J_I}{206,300 H_F} \omega_E^2 \delta_{TE}^2 \cos 2\alpha] \sin 2k\theta_n \\
& + [D_S \cos \lambda - 1/2 D_{OS} \sin 2\lambda + \omega_E \delta_{TE} (\cos \alpha + \zeta_O \sin \alpha)]
\end{aligned}$$

$$\begin{aligned}
& + \frac{J_S - J_I}{206,300 H_f} \omega_E^2 (1+b) \delta_{OST} \delta_{TE} \sin(\alpha - \beta_2)] \cos k\theta_n \\
& + 1/2 [(D_{II} - D_{SS}) \cos^2 \lambda + \frac{J_S - J_I}{206,300 H_f} \omega_E^2 \delta_{TE}^2 \sin 2\alpha] \cos 2k\theta_n
\end{aligned} \tag{5-9}$$

5.4.2.2 Clockwise Rotation of the Table: The setup is the same as in Fig. 5-3, but the table is now rotated in the clockwise direction without disturbing the setup used for the counterclockwise rotation of the table. The command rate-to-balance equation is the same as Eq. (5-9), except that $(1+b)$ is replaced by $(1-b)$, and the command rate-to-balance current is i'_{OSk} at table angle $\theta_k = k\theta_n$. The table angle θ is still measured in a counterclockwise direction from west as shown in Fig. 5-3(a).

5.4.2.3 Weighting the Data from Position No. 2: In order to eliminate some of the effects of the gyro misalignment angle δ_{OST} and to minimize other misalignment effects, we will weight the data as follows:

$$\begin{aligned}
W_{OSk} &= \frac{K_T}{2b} [(b-1) i_{OSk} + (b+1) i'_{OSk}] \\
&= -[D_F - D_O \sin \lambda + D_{OO} \sin^2 \lambda + 1/2(D_{II} + D_{SS}) \cos^2 \lambda \\
&\quad + \frac{J_S - J_I}{412,600 H_f} \omega_E^2 (b^2 - 1) \delta_{OST}^2 \sin 2\beta_2] + [D_I \cos \lambda \\
&\quad - 1/2 D_{IO} \sin 2\lambda + \omega_E \delta_{TE} (\sin \alpha - \zeta_O \cos \alpha)] \sin k\theta_n \\
&\quad - 1/2 [D_{IS} \cos^2 \lambda + \frac{J_S - J_I}{206,300 H_f} \omega_E^2 \delta_{TE}^2 \cos 2\alpha] \sin 2k\theta_n \\
&\quad + [D_S \cos \lambda - 1/2 D_{OS} \sin 2\lambda \\
&\quad + \omega_E \delta_{TE} (\cos \alpha + \zeta_O \sin \alpha)] \cos k\theta_n + 1/2 [(D_{II} - D_{SS}) \cos^2 \lambda \\
&\quad + \frac{J_S - J_I}{206,300 H_f} \omega_E^2 \delta_{TE}^2 \sin 2\alpha] \cos 2k\theta_n
\end{aligned} \tag{5-10}$$

5.4.3 Control of Misalignment Errors

It is somewhat easier to investigate the impact of the misalignment errors if we look at the sum and difference of Eqs. (5-6) and (5-10).

$$\begin{aligned}
 W_{ONk} + W_{OSk} = & -[2D_F + 2D_{OO} \sin^2 \lambda + (D_{II} + D_{SS}) \cos^2 \lambda \\
 & + \frac{J_S - J_I}{412,600 H_r} \omega_E^2 (b^2 - 1) (\delta_{ONT}^2 \sin 2\beta_1 + \delta_{OST}^2 \sin 2\beta_2)] \\
 & - [D_{IO} \sin 2\lambda + 2 \omega_E \delta_{TE} \zeta_O \cos \alpha] \sin k\theta_n \\
 & + 2[D_S \cos \lambda + \omega_E \delta_{TE} \zeta_O \sin \alpha] \cos k\theta_n \\
 & + (D_{II} - D_{SS}) \cos^2 \lambda \cos 2k\theta_n
 \end{aligned} \tag{5-11}$$

$$\begin{aligned}
 W_{ONk} - W_{OSk} = & -[2D_O \sin \lambda + \frac{J_S - J_I}{412,600 H_r} \omega_E^2 (b^2 - 1) (\delta_{ONT}^2 \sin 2\beta_1 \\
 & - \delta_{OST}^2 \sin 2\beta_2)] - 2[D_I \cos \lambda + \omega_E \delta_{TE} \sin \alpha] \sin k\theta_n + [D_{IS} \cos^2 \lambda \\
 & + \frac{J_S - J_I}{206,300 H_r} \omega_E^2 \delta_{TE}^2 \cos 2\alpha] \sin 2k\theta_n + [D_{OS} \sin 2\lambda \\
 & - 2 \omega_E \delta_{TE} \cos \alpha] \cos k\theta_n - \frac{J_S - J_I}{206,300 H_r} \omega_E^2 \delta_{TE}^2 \sin 2\alpha \cos 2k\theta_n
 \end{aligned} \tag{5-12}$$

It is easier, in general, to control the misalignment of the table axis to the earth axis (angle δ_{TE}) than it is to control the misalignment of the gyro output reference axis with respect to the table axis (angles δ_{ONT} and δ_{OST}). The latter misalignment angles result from manufacturing and assembly tolerances of the gyro, the mounting fixture and the table. In addition, those angles may be a function of the clamping loads, the average temperature, and the temperature gradients in the test setup and in the gyro.

It is relatively easy to control δ_{TE} to less than 0.001 rad ($\approx 3 \text{ min}$), and it may be controlled as closely as 15×10^{-6} rad ($\approx 3 \text{ sec}$) on a very stable pier.

The misalignment angle ζ_O in a well-designed and assembled gyro should be less than 0.01 rad ($\approx 34 \text{ min}$); therefore, if we control $\omega_E \delta_{TE}$ in Eq. (5-12) to a satisfactory degree, then the error terms containing $\omega_E \delta_{TE} \zeta_O$ in Eq. (5-11) should be quite negligible and may be deleted.

At a latitude of 45° , it is seen that $\omega_E \delta_{TE}$ must be less than 7% of D_I and 5% of D_{OS} if these coefficients are to be determined with an error of less than 10%. For example, if $D_{OS} = 0.001 \omega_E$, then $2 \omega_E \delta_{TE}$ must be less than $0.1 \times 0.001 \omega_E$ or δ_{TE} must be less than $1 \times 10^{-4} / 2 = 5 \times 10^{-5}$ rad ($\approx 10 \text{ sec}$) if D_{OS} is to be determined with an error of less than 10%. It is obviously far more difficult to determine D_{OS} or D_I accurately if they are only $1 \times 10^{-4} \omega_E$, though some manufacturers make even more doubtful claims.

Let us now look at the remaining error terms; these involve the ratio $(J_S - J_I)/H_r$. Since in general, the misalignment angles δ_{ONT} and δ_{OST} would be greater than δ_{TE} and $(b^2 - 1) \gg 1$, then the errors in the constant terms of the Fourier expansions are more significant than the errors in the other Fourier coefficients. The Central Inertial Guidance Test Facility at Holloman AFB normally performs its tests with $b = 20$ and, on occasion, as high as $b = 100$. Let us look at the order of magnitude of these errors by assuming some values for the various parameters which will give errors greater than what would ordinarily be expected. Let $J_S - J_I = 1000 \text{ gm} \cdot \text{cm}^2$, $H_r = 10^4 \text{ gm} \cdot \text{cm}^2/\text{s}$, $\delta_{ONT} = \delta_{OST} = 0.05 \text{ rad}$, $\sin 2\beta_1 = \sin 2\beta_2 = 0.5$, $b = 100$, and $\omega_E = 15 \text{ deg/hr}$. Then,

$$\frac{J_S - J_I}{412,600 H_r} \omega_E^2 (b^2 - 1) (\delta_{ONT}^2 \sin 2\beta_1 + \delta_{OST}^2 \sin 2\beta_2) =$$

$$\frac{1000}{412,600 \times 10,000} \times 225 \times 10,000 (0.0025 \times 0.5$$

$$+ 0.0025 \times 0.5) = 0.0014 \text{ deg/hr}$$

Therefore, even with these rather extreme values, the error would be negligible in most applications. However, it would be well to estimate this error for each new design and test setup in order to confirm that it is negligible. If the error is not negligible, there are several steps we may take to reduce it; they are: a) apply closer tolerances on the manufacture and assembly of the gyro, b) apply closer tolerances on the manufacture and assembly of the mounting fixture, c) correct any non-orthogonality of the table face to the table axes, d) use a lower table rate, e) increase the angular momentum of the gyro and/or decrease $J_S - J_I$.

5.4.4 Gyro Coefficients from OA \rightarrow North and OA \rightarrow South Tests

If we assume that the misalignment terms of Eqs. (5-11) and (5-12) are controlled and negligible compared to the gyro coefficients, as is necessary, and we now apply the method of least squares to Eqs. (5-11) and (5-12), then the following equations are obtained:

$$2 D_F + 2 D_{OO} \sin^2 \lambda + (D_{II} + D_{SS}) \cos^2 \lambda = \frac{-1}{n} \sum_{k=1}^n (W_{ONk} + W_{OSk})$$

$$D_{IO} = \frac{-2}{n \sin 2\lambda} \sum_{k=1}^n (W_{ONk} + W_{OSk}) \sin k\theta_n$$

$$D_S = \frac{1}{n \cos \lambda} \sum_{k=1}^n (W_{ONk} + W_{OSk}) \cos k\theta_n$$

$$D_{II} - D_{SS} = \frac{2}{n \cos^2 \lambda} \sum_{k=1}^n (W_{ONk} + W_{OSk}) \cos 2k\theta_n$$

$$D_O = \frac{-1}{2n \sin \lambda} \sum_{k=1}^n (W_{ONk} - W_{OSk})$$

$$D_I = \frac{-1}{n \cos \lambda} \sum_{k=1}^n (W_{ONk} - W_{OSk}) \sin k\theta_n$$

$$D_{IS} = \frac{2}{n \cos^2 \lambda} \sum_{k=1}^n (W_{ONk} - W_{OSk}) \sin 2k\theta_n$$

$$D_{OS} = \frac{2}{n \sin^2 \lambda} \sum_{k=1}^n (W_{ONk} - W_{OSk}) \cos k\theta_n \quad (5-13)$$

Since there are only two equations involving the four unknown coefficients D_F , D_{II} , D_{OO} , and D_{SS} , it is necessary to obtain two more independent equations involving D_F and at least one of the other three coefficients, or make some simplifying assumptions.

Some organizations assume that $D_{OO} = 0$, in which case only one more independent equation is required. An additional tumble test with SRA parallel to the earth's polar axis will provide the necessary relationship. The equations for such a tumble test are derived in a manner similar to that used for Positions Nos. 1 and 2. Unfortunately, a new misalignment error term appears which involves J_O/H_F . These errors are probably negligible in most cases, but if not, they are not so readily amenable to minimization by design changes.

Other organizations assume that D_{OO} and either D_{II} or D_{SS} are zero. Equations (5-13) are then sufficient to determine all the remaining coefficients. The assumption that $D_{OO} = 0$ is justifiable on the somewhat weak grounds that no theoretical analyses have shown a need for such a term. However, it is difficult to justify setting either D_{II} or D_{SS} equal to zero, and certainly not one in preference to the other.

The most accurate method for obtaining the quadratic and cross-coupled coefficients, such as D_{II} and D_{OS} , is on a precision linear shaker. The common electromagnetic shakers, used either with or without a slip table, are not usually satisfactory since they may have substantial cross axis and angular motions. This technique will be analyzed in Section 6. We will now turn to the discrete position tumble test.

5.5 Discrete Position Tumble Test

In the discrete position tumble test, the command rate-to-balance current is measured at a series of table positions after equilibrium has been reached. Thus, some of the dynamic error terms are avoided, but of course, other errors appear.

5.5.1 Position No. 1, ORA → North

The mounting position is identical to that described in Section 5.4.1 for the continuous rotation tumble test. The command rate-to-balance current is measured at table angles $\theta_k = k\theta_n$ where $\theta_n = 360^\circ/n$ and $k = 1, 2, 3, \dots, n$. The results are the same as given by Eq. (5-5) with $b = 0$. The gyro must be allowed to attain equilibrium at each table angle.

$$\begin{aligned}
 K_{T^i ONk} = & -[D_F + D_O \sin \lambda + D_{OO} \sin^2 \lambda + 1/2(D_{II} + D_{SS}) \cos^2 \lambda \\
 & + \omega_E \delta_{ONT} (\cos \beta_1 - \zeta_O \sin \beta_1) \\
 & + \frac{J_S - J_I}{412,600 H_F} \omega_E^2 \delta_{ONT}^2 \sin 2\beta_1] \\
 & - [D_I \cos \lambda + 1/2 D_{IO} \sin 2\lambda + \omega_E \delta_{TE} (\sin \alpha + \zeta_O \cos \alpha) \\
 & - \frac{J_S - J_I}{206,300 H_F} \omega_E^2 \delta_{ONT} \delta_{TE} \cos(\alpha + \beta_1)] \sin k\theta_n \\
 & + 1/2 [D_{IS} \cos^2 \lambda + \frac{J_S - J_I}{206,300 H_F} \omega_E^2 \delta_{TE}^2 \cos 2\alpha] \sin 2k\theta_n \\
 & + [D_S \cos \lambda + 1/2 D_{OS} \sin 2\lambda - \omega_E \delta_{TE} (\cos \alpha - \zeta_O \sin \alpha) \\
 & - \frac{J_S - J_I}{206,300 H_F} \omega_E^2 \delta_{ONT} \delta_{TE} \sin(\alpha + \beta_1)] \cos k\theta_n
 \end{aligned}$$

$$\begin{aligned}
& + 1/2 [D_{II} - D_{SS}) \cos^2 \lambda \\
& - \frac{J_S - J_I}{206,300 H_F} \omega_E^2 \delta_{TE}^2 \sin 2\alpha] \cos 2k\theta_n \quad (5-14)
\end{aligned}$$

Unlike the continuous tumble tests, it makes no difference, theoretically, whether the table is rotated clockwise or counterclockwise from one table angle to the next, providing equilibrium conditions are attained at each table angle before readings are taken, and providing there is no hysteresis due to pivot friction or other causes. If hysteresis effects are suspected, then readings should be taken in both clockwise and counterclockwise rotation. The rotation from one position to another should be smooth and unidirectional.

5.5.2 Position No. 2, ORA → South

The mounting position is identical to that described in Section 5.4.2. The command rate-to-balance current is measured at table angles $\theta_k = k\theta_n$, where $\theta_n = 360^\circ/n$ and $k = 1, 2, 3, \dots, n$. The results are the same as given by Eq. (5-9) with $b = 0$. The same cautions regarding equilibrium and hysteresis given in Section 5.5.1 also apply here.

$$\begin{aligned}
K_{T^1 OSk} = & -[D_F - D_O \sin \lambda + D_{OO} \sin^2 \lambda + 1/2(D_{II} + D_{SS}) \cos^2 \lambda \\
& + \omega_E \delta_{OST} (\cos \beta_2 - \zeta_O \sin \beta_2) \\
& + \frac{J_S - J_I}{412,600 H_F} \omega_E^2 \delta_{OST}^2 \sin 2\beta_2] + [D_I \cos \lambda \\
& - 1/2 D_{IO} \sin 2\lambda + \omega_E \delta_{TE} (\sin \alpha - \zeta_O \cos \alpha) \\
& + \frac{J_S - J_I}{206,300 H_F} \omega_E^2 \delta_{OST} \delta_{TE} \cos(\alpha + \beta_2)] \sin k\theta_n
\end{aligned}$$

$$\begin{aligned}
& - 1/2 [D_{IS} \cos^2 \lambda + \frac{J_S - J_I}{206,300 H_F} \omega_E^2 \delta_{TE}^2 \cos 2\alpha] \sin 2k\theta_n \\
& + [D_S \cos \lambda - 1/2 D_{OS} \sin 2\lambda + \omega_E \delta_{TE} (\cos \alpha + \zeta_O \sin \alpha) \\
& + \frac{J_S - J_I}{206,300 H_F} \omega_E^2 \delta_{OST} \delta_{TE} \sin(\alpha - \beta_2)] \cos k\theta_n \\
& + 1/2 [(D_{II} - D_{SS}) \cos^2 \lambda + \frac{J_S - J_I}{206,300 H_F} \omega_E^2 \delta_{TE}^2 \sin 2\alpha] \cos 2k\theta_n
\end{aligned} \tag{5-15}$$

5.5.3

Gyro Coefficients from OA → North and OA → South Tests

The sum and difference of Eqs. (5-14) and (5-15) are:

$$\begin{aligned}
K_T(i_{ONk} + i_{OSk}) = & -[2D_F + 2D_{OO} \sin^2 \lambda + (D_{II} + D_{SS}) \cos^2 \lambda \\
& + \omega_E \delta_{ONT} (\cos \beta_1 - \zeta_O \sin \beta_1) \\
& + \omega_E \delta_{OST} (\cos \beta_2 - \zeta_O \sin \beta_2) \\
& + \frac{J_S - J_I}{412,600 H_F} \omega_E^2 (\delta_{ONT}^2 \sin 2\beta_1 + \delta_{OST}^2 \sin 2\beta_2)] \\
& - [D_{IO} \sin 2\lambda + 2\omega_E \delta_{TE} \zeta_O \cos \alpha \\
& - \frac{J_S - J_I}{206,300 H_F} \omega_E^2 \delta_{TE} [\delta_{ONT} \cos(\alpha + \beta_1) \\
& + \delta_{OST} \cos(\alpha + \beta_2)]] \sin k\theta_n \\
& + [2D_S \cos \lambda + 2\omega_E \delta_{TE} \zeta_O \sin \alpha \\
& - \frac{J_S - J_I}{206,300 H_F} \omega_E^2 \delta_{TE} [\delta_{ONT} \sin(\alpha + \beta_1) \\
& - \delta_{OST} \sin(\alpha - \beta_2)]] \cos k\theta_n + (D_{II} - D_{SS}) \cos^2 \lambda \cos 2k\theta_n
\end{aligned} \tag{5-16}$$

$$\begin{aligned}
K_T(i_{ONk} - i_{OSk}) = & - [2D_O \sin \lambda + \omega_E \delta_{ONT} (\cos \beta_1 - \zeta_O \sin \beta_1) \\
& - \omega_E \delta_{OST} (\cos \beta_2 - \zeta_O \sin \beta_2) + \frac{J_S - J_I}{412,600 H_F} \omega_E^2 (\delta_{ONT}^2 \sin 2\beta_1 \\
& - \delta_{OST}^2 \sin 2\beta_2)] - [2 D_I \cos \lambda + 2 \omega_E \delta_{TE} \sin \alpha \\
& + \frac{J_S - J_I}{206,300 H_F} \omega_E^2 \delta_{TE} [\delta_{ONT} \cos(\alpha + \beta_1) \\
& - \delta_{OST} \cos(\alpha + \beta_2)] \sin k\theta_n \\
& + [D_{IS} \cos^2 \lambda + \frac{J_S - J_I}{206,300 H_F} \omega_E^2 \delta_{TE}^2 \cos 2\alpha] \sin 2k\theta_n \\
& + [D_{OS} \sin 2\lambda - 2 \omega_E \delta_{TE} \cos \alpha \\
& - \frac{J_S - J_I}{206,300 H_F} \omega_E^2 \delta_{TE} [\delta_{ONT} \sin(\alpha + \beta_1) \\
& + \delta_{OST} \sin(\alpha - \beta_2)] \cos k\theta_n \\
& - \frac{J_S - J_I}{206,300 H_F} \omega_E^2 \delta_{TE}^2 \sin 2\alpha \cos 2k\theta_n] \quad (5-17)
\end{aligned}$$

The discussion in Section 5.4.3 on the error terms containing $(J_S - J_I)/H_F$ would also apply here, except that the errors are usually negligible since they are not multiplied by $(b^2 - 1)$. It is obvious that any remaining error terms containing products of misalignment angles are very easily controlled and may also be neglected. Neglecting those terms, Eqs. (5-16) and (5-17) reduce to:

$$\begin{aligned}
K_T(i_{ONk} + i_{OSk}) = & - [2D_F + 2D_{OO} \sin^2 \lambda + (D_{II} + D_{SS}) \cos^2 \lambda \\
& + \omega_E (\delta_{ONT} \cos \beta_1 + \delta_{OST} \cos \beta_2)] - D_{IO} \sin 2\lambda \sin k\theta_n
\end{aligned}$$

$$+ 2D_S \cos \lambda \cos k\theta_n + (D_{II} - D_{SS}) \cos^2 \lambda \cos 2k\theta_n \quad (5-18)$$

$$\begin{aligned} K_T(i_{ONk} - i_{OSk}) = & -[2D_O \sin \lambda + \omega_E (\delta_{ONT} \cos \beta_1 - \delta_{OST} \cos \beta_2)] \\ & - 2(D_I \cos \lambda + \omega_E \delta_{TE} \sin \alpha) \sin k\theta_n + D_{IS} \cos^2 \lambda \sin 2k\theta_n \\ & + (D_{OS} \sin 2\lambda - 2\omega_E \delta_{TE} \cos \alpha) \cos k\theta_n \end{aligned} \quad (5-19)$$

Knowing the desired accuracy for the performance coefficients, it is relatively easy to control the misalignment angle δ_{TE} to the required magnitude. Unfortunately, the terms $\omega_E \delta_{ONT} \cos \beta_1$ and $\omega_E \delta_{OST} \cos \beta_2$ are not as amenable to control and cannot be eliminated by weighting clockwise and counterclockwise rotation as is done in continuous rotation tumble tests. A careful estimate of the maximum error must be made and compared to the allowable error. The misalignment angles include misalignment of the gyro to the table axis, non-orthogonality of table face to table axis, mounting fixture errors, effects of bolting torques, and dirt on mounting surfaces.

Assuming the misalignment errors have been properly controlled, we may apply the method of least squares to Eqs. (5-18) and (5-19). The resulting normal equations are:

$$2D_F + 2D_{OO} \sin^2 \lambda + (D_{II} + D_{SS}) \cos^2 \lambda = \frac{-K_T}{n} \sum_{k=1}^n (i_{ONk} + i_{OSk})$$

$$D_{IO} \sin 2\lambda = \frac{-2K_T}{n} \sum_{k=1}^n (i_{ONk} + i_{OSk}) \sin k\theta_n$$

$$D_S \cos \lambda = \frac{K_T}{n} \sum_{k=1}^n (i_{ONk} + i_{OSk}) \cos k\theta_n$$

$$(D_{II} - D_{SS}) \cos^2 \lambda = \frac{2K_T}{n} \sum_{k=1}^n (i_{ONk} + i_{OSk}) \cos 2k\theta_n$$

$$D_O \sin \lambda = \frac{-K_T}{2n} \sum_{k=1}^n (i_{ONk} - i_{OSk})$$

$$D_I \cos \lambda = \frac{-K_T}{n} \sum_{k=1}^n (i_{ONk} - i_{OSk}) \sin k\theta_n$$

$$D_{IS} \cos^2 \lambda = \frac{2K_T}{n} \sum_{k=1}^n (i_{ONk} - i_{OSk}) \sin 2k\theta_n$$

$$D_{OS} \sin 2\lambda = \frac{2K_T}{n} \sum_{k=1}^n (i_{ONk} - i_{OSk}) \cos k\theta_n$$

As with the continuous rotation tumble test, there are ten unknown coefficients, but only eight equations. This leads to the need for two more independent equations or for some simplifying assumptions. Refer to Section 5.4.4 for a discussion of this subject.

6. PRECISION LINEAR VIBRATION TEST

6.1 Introduction

As previously mentioned, the most accurate method of obtaining the coefficients of the quadratic and cross-coupling terms such as D_{II} and D_{IS} , is on a precision linear vibration table. The great advantage of the vibration test over the tumble test is due to the higher acceleration level available which greatly magnifies the response because the drift rate varies as the square of the input acceleration. Since it is the quasi-static value of each coefficient that is generally desired, care must be taken to have the input frequency well below any resonant frequency of the gyro or of the mounting fixture. In research and development, it is probably desirable to test at more than one frequency.

Mounting the gyro and its fixture directly on the ordinary electromagnetic shaker, or on an ordinary slip table driven by such a shaker, is often not acceptable because of the large components of cross acceleration and angular acceleration which are usually present. A precision linear shaker such as the one in the Charles Stark Draper Laboratory, driving a good Team table is required.

In order to minimize the effects of earth's rate, the vibration input should be along a line normal to the polar axis such as a horizontal east-west line, and IA should be normal to the polar axis whenever possible. We will assume that reasonable care has been taken in the setup and mounting of the gyro so that the total misalignments of the gyro axes, as mounted with respect to the vibration axis, earth axis, and the gravity vector are less than 0.01 rad ($\approx 34 \text{ min}$) and may be neglected.

The determination of only three coefficients will be illustrated in the following sections; all others may be determined in a similar method.

6.2

Determination of D_{II} - Position No. 1

Mount the gyro on the precision linear shaker with ORA pointing north along the earth's axis EA, and IRA pointing east as shown in Fig. 6-1. The line H-H represents the horizon, λ is the astronomic latitude, and a_v is the vibration input in g units with amplitude A_{1k} (0 to peak).

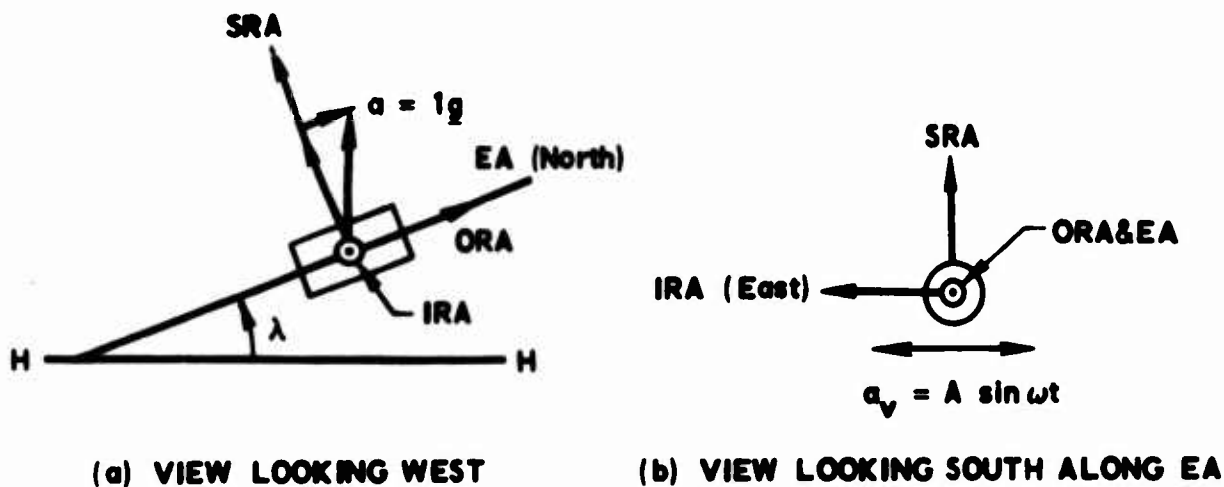


Fig. 6-1. Gyro Axes in Vibration Position No. 1

The gyro is vibrated at $(n+1)$ different acceleration amplitudes A_{1k} , $k=0, 1, 2, \dots, n$, and $A_{10} = 0$. The components of acceleration and earth rate along the gyro axes in Position No. 1 are:

$$a_{IIk} = A_{1k} \sin \omega t$$

$$a_{OIk} = \sin \lambda$$

$$a_{SIk} = \cos \lambda$$

$$\omega_{IE} \approx \omega_{SE} \approx 0$$

$$\omega_{OE} = \omega_E$$

(6-1)

Substitute Eqs. (6-1) and (6-2) in Eq. (4-2) and let i_{1k} be the command rate-to-balance current in Position No. 1 at vibration amplitude A_{1k} .

$$\begin{aligned} W_{11k} = K_T i_{1k} = & -[D_F + D_I A_{1k} \sin \omega t + D_O \sin \lambda + D_S \cos \lambda \\ & + D_{II} A_{1k}^2 \sin^2 \omega t + D_{OO} \sin^2 \lambda + D_{SS} \cos^2 \lambda \\ & + D_{IO} A_{1k} \sin \lambda \sin \omega t + D_{OS} \sin \lambda \cos \lambda + D_{IS} \cos \lambda A_{1k} \sin \omega t] \end{aligned}$$

The average command rate-to-balance over a time interval NT , where N is an integer and $T = 2\pi/\omega$ is the period of the vibration, is:

$$\begin{aligned} \bar{W}_{11k} = \frac{K_T}{NT} \int_0^{NT} i_{1k} dt = & -[D_F + D_O \sin \lambda + D_S \cos \lambda + 1/2 D_{II} A_{1k}^2 \\ & + D_{OO} \sin^2 \lambda + D_{SS} \cos^2 \lambda + D_{OS} \sin \lambda \cos \lambda] \end{aligned} \quad (6-3)$$

Perform the above test for $k = 1, 2, 3, \dots, n$. In testing a new model of a gyro or a gyro mounted on a new fixture, it is good practice to test at several frequencies in order to ascertain that the final test runs are not performed near or beyond any resonant frequency of gyro or mount.

Without disturbing the setup in any manner, determine the average command rate-to-balance current with $A_{1k} = A_{10} = 0$. The average command rate-to-balance is:

$$\begin{aligned} W_{110} = \frac{K_T}{NT} \int_0^{NT} i_{10} dt = & -[D_F + D_O \sin \lambda + D_S \cos \lambda + D_{OO} \sin^2 \lambda \\ & + D_{SS} \cos^2 \lambda + D_{OS} \sin \lambda \cos \lambda] \end{aligned} \quad (6-4)$$

Subtract Eq. (6-4) from Eq. (6-3) for each input acceleration level, sum the results, and solve for D_{II} .

$$D_{II} \sum_{k=1}^n A_{1k}^2 = 2n \bar{W}_{II0} - 2 \sum_{k=1}^n \bar{W}_{IIk} \quad (6-5)$$

It is often useful to plot the change in indicated command rate ($\bar{W}_{IIk} - \bar{W}_{II0}$) versus input acceleration level squared. This relationship should be linear, and the slope is proportional to D_{II} .

6.3 Determination of D_{SS} - Position No. 2

Rotate the gyro 90° about ORA to Position No. 2, as shown in Fig. 6-2.

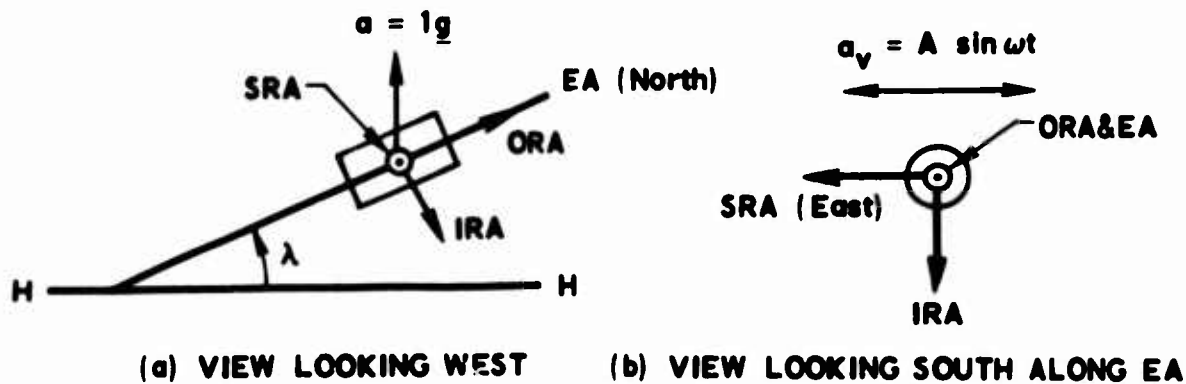


Fig. 6-2. Gyro Axes in Vibration Position No. 2

Perform the vibration tests at n amplitude levels A_{2k} (not necessarily the same levels used in Position No. 1, except that $A_{20} = A_{10} = 0$). The components of acceleration and earth rate along the gyro axes are:

$$\begin{aligned} a_{I2k} &= -\cos\lambda \\ a_{O2k} &= \sin\lambda \\ a_{S2k} &= A_{2k} \sin \omega t \end{aligned} \quad (6-6)$$

$$\begin{aligned} \omega_{IE} &\approx \omega_{SE} \approx 0 \\ \omega_{OE} &\approx \omega_E \end{aligned} \quad (6-7)$$

Substitute Eqs. (6-6) and (6-7) in Eq. (4-2) and reduce the data in a manner similar to the methods used in Section 6.2.

$$D_{SS} \sum_{k=1}^n A_{2k}^2 = 2n \bar{W}_{I2O} - 2 \sum_{k=1}^n \bar{W}_{I2k} \quad (6-8)$$

6.4 Determination of D_{IS} - Position No. 3

Rotate the gyro about ORA to the position shown in Fig. 6-3.

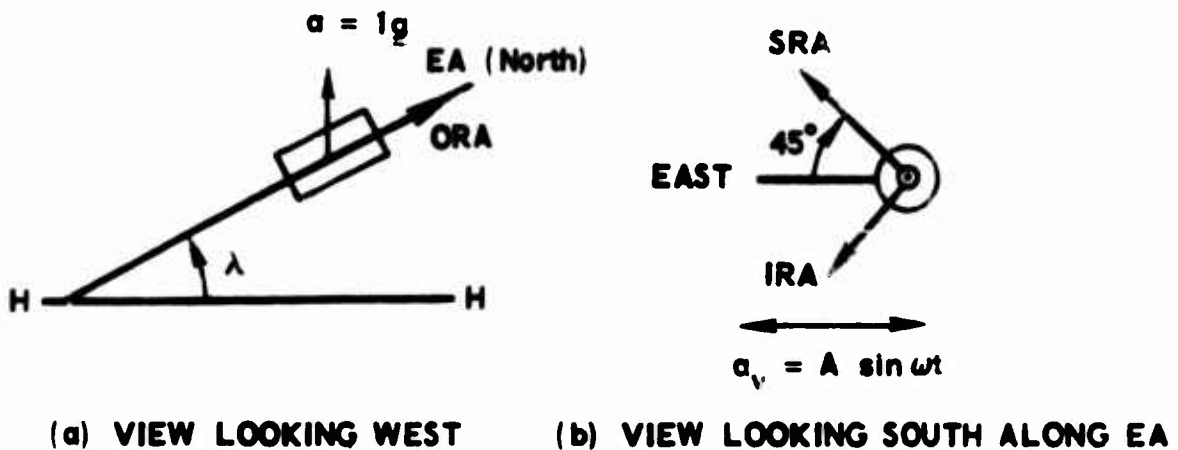


Fig. 6-3. Gyro Axes in Vibration Position No. 3

The components of acceleration and of earth rate along the gyro axes are:

$$\begin{aligned} a_{I3k} &= -\frac{\sqrt{2}}{2} \cos \lambda + \frac{\sqrt{2}}{2} A_{3k} \sin \omega t \\ a_{O3k} &= \sin \lambda \\ a_{S3k} &= \frac{\sqrt{2}}{2} \cos \lambda + \frac{\sqrt{2}}{2} A_{3k} \sin \omega t \end{aligned} \quad (6-9)$$

$$\omega_{IE} = \omega_{SE} \approx 0$$

$$\omega_{OE} = \omega_E \quad (6-10)$$

Again, take data at each amplitude level A_{3k} , including $A_{30} = 0$. Applying the same data reduction procedure as before, we find:

$$(D_{II} + D_{SS} + D_{IS}) \sum_{k=1}^n A_{3k} = 4n \bar{W}_{I30} - 4 \sum_{k=1}^n \bar{W}_{I3k} \quad (6-11)$$

One could substitute the values of D_{II} and D_{SS} obtained from Eqs. (6-5) and (6-8) in Eq. (6-11) and solve for D_{IS} . Because of the standard errors of the mean values of D_{II} and D_{SS} , it is a somewhat better procedure to rotate the gyro 90° about ORA from position 3 and perform another series of vibration runs with the vibration inputs along IRA and SRA being 180° out of phase. The reduced equation for this fourth position is:

$$(D_{II} + D_{SS} - D_{IS}) \sum_{k=1}^n A_{4k}^2 = 4n \bar{W}_{I40} - 4 \sum_{k=1}^n \bar{W}_{I4k} \quad (6-12)$$

The value of D_{IS} is obtained from Eqs. (6-11) and (6-12). The coefficients D_{IO} and D_{OS} may be determined in a similar manner.

7. TORQUES DUE TO DENSITY GRADIENTS

If the gyro fluid has a density gradient along an axis normal to the output axis, and if there is an applied acceleration component normal to both the gradient axis and the output axis, then convection currents will be generated which will exert a torque about the output axis with resulting drift rate about the input axis. The density gradient may result from a temperature gradient and/or stratification of a non-homogeneous fluid. Most gyro fluids are polymers containing a range of molecular weights and are nearly, but not quite, homogeneous.

The fluid flow must be determined from the partial differential equations of potential flow theory. Except for the very simplest cases, these equations must be solved by numerical integration methods. There are many possible density gradients occurring in gyros; we will consider one simple example.

Let us assume that the gimbal is a right circular cylinder, and that the fluid density varies linearly along the spin axis as expressed by Eq. (7-1) and indicated in Fig. 7-1(a).

$$\rho_{\theta} = \rho_0 \left[1 + \frac{\Delta\rho}{2\rho_0} \frac{x}{R} \right] = \rho_0 \left[1 + \frac{\Delta\rho}{2\rho_0} \sin\theta \right] \quad (7-1)$$

where

ρ_{θ} = fluid density at angle θ - g/cm³

ρ_0 = fluid density at $\theta = 0^\circ$ - g/cm³

$\Delta\rho = \rho_{90} - \rho_{270}$ - g/cm³

x = distance along SA from origin - cm

R = radius of gimbal - cm

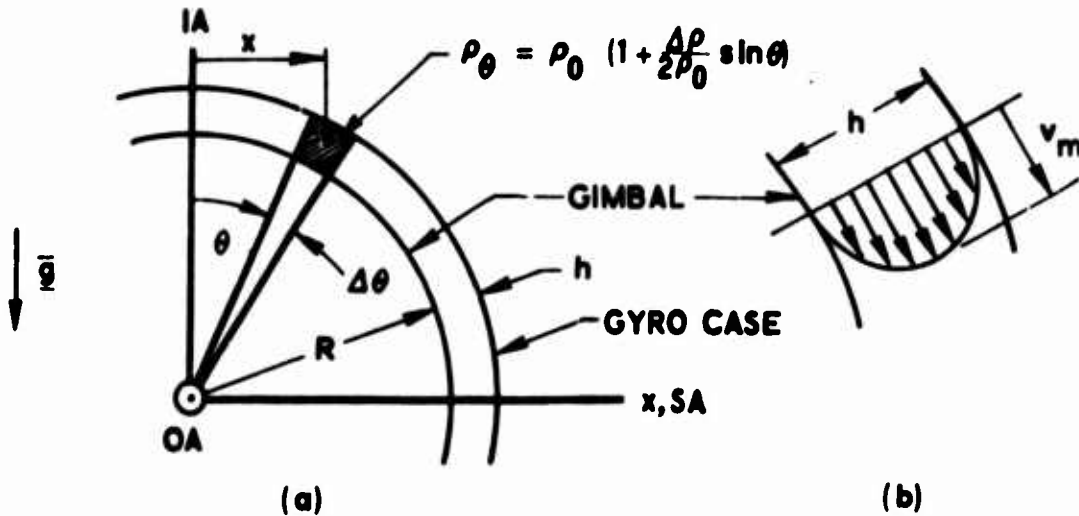


Fig. 7-1. Density Distribution and Fluid Flow

Assume that the fluid gap h is very much smaller than the radius R , which is true in all such gyros, and that the density of the fluid is essentially uniform in the cross-hatched volume enclosed by the small angle $\Delta\theta$, gap h , and gimbal length l . Let the gyro be fixed to the earth with IA up, i. e., gravity vector \bar{g} is acting downward as shown in Fig. 7-1(a).

Rather than solve the potential flow equations which would require tedious numerical methods, we will determine only the initial torque exerted on the gimbal. This is not really such a great shortcoming, since it is known from other considerations that the time constant for the convection flow in a one- g field is many hours or even several days.

With the above conditions, in particular the narrow fluid gap, the initial velocity distribution will be nearly parabolic (approaches parallel plate conditions), as indicated in Fig. 7-1(b). In addition, continuity requires that the initial velocity distribution across the gap be the same all around the circumference.

The moment of the fluid weight about OA is

$$M_W = -Ghl R^2 \rho_0 \int_0^{2\pi} \left(1 + \frac{\Delta\rho}{2\rho_0} \sin\theta\right) \sin\theta d\theta$$

or

$$M_W = \frac{-\pi}{2} Gh l R^2 \Delta\rho \quad (7-2)$$

where

M_W = moment of fluid weight - dyn·cm

G = local value of gravity - cm/s²

l = length of gimbal - cm

With a parabolic velocity distribution across the gap, the viscous drag per unit area on either the gimbal or the gyro case is

$$F_D = \frac{4\mu v_m}{h} = \frac{6\mu v_a}{h} \quad (7-3)$$

where

F_D = drag per unit area at interface - dyn/cm²

μ = viscosity - poise = dyn·s/cm²

v_m = maximum fluid velocity - cm/s

v_a = average fluid velocity - $2v_m/3$ - cm/s

Formula (7-3) may be found in any fluid mechanics textbook for forced flow between parallel plates.

The total viscous drag moment exerted by the gimbal and the gyro case on the fluid is

$$M_\mu = 2(2\pi R l) F_D \cdot R = \frac{24\mu \pi R^2 l}{h} v_a \quad (7-4)$$

Because of the extremely low fluid velocity, we may neglect the inertia of the fluid. Then, for equilibrium of the fluid, we have:

$$M_W + M_\mu = 0 = -\frac{\pi}{2} Gh l R^2 \Delta \rho + \frac{24\mu \pi R^2 l}{h} v_a$$

or

$$v_a = \frac{Gh^2 \Delta \rho}{48\mu} \quad (7-5)$$

The viscous drag moment acting on the gimbal about OA is:

$$M_{\mu O} = -M_\mu / 2 \quad (7-6)$$

Substitute Eqs. (7-4) and (7-5) in (7-6).

$$M_{\mu O} = \frac{-\pi}{4} Gh l R^2 \Delta \rho \text{ dyn} \cdot \text{cm} \quad (7-7)$$

Notice that the moment exerted on the gimbal is independent of the viscosity of the fluid. However, the time constant is dependent on the viscosity.

The resulting drift rate about the input axis is:

$$\omega_I = -\frac{M_{\mu O}}{H_r} \text{ rad/sec} = -206,300 \frac{M_{\mu O}}{H_r} \text{ deg/hr}$$

or

$$\omega_I = 206,300 \frac{\pi}{4H_r} Gh l R^2 \Delta \rho = 162,000 Gh l R^2 \frac{\Delta \rho}{H_r} \frac{\text{deg}}{\text{hr}} \quad (7-8)$$

where

$$H_r = \text{rotor angular momentum} - \text{gm} \cdot \text{cm}^2 / \text{s}$$

Example

Determine the maximum drift rate of a gyro fixed to earth with OA horizontal and IA vertical if the fluid density varies linearly along the spin axis. The gyro has the following parameters:

$H_r = 34,000 \text{ gm} \cdot \text{cm}^2 / \text{s}$	$\rho_0 = 2.36 \text{ gm/cm}^3$
$h = 0.020 \text{ cm}$	$\Delta \rho = 0.001 \rho_0$
$R = 1.5 \text{ cm}$	$\mu = 7.92 \text{ poises}$
$l = 2.5 \text{ cm}$	$G = 981 \text{ cm/s}^2$

$$\omega_I = 162,000 \times 981 \times 0.02 \times 2.5 \times 1.5^2 \times \frac{0.00236}{34,000}$$

$$\omega_I = 1.24 \text{ deg/hr}$$

Even if the gyro fluid was monomolecular, which is not generally true, it would require a temperature gradient of only slightly more than one degree to obtain this rather large drift rate in a one-g field.

The average velocity of the fluid in the gap may be determined from Eq. (7-5)

$$v_a = \frac{981 \times 0.02^2 \times 0.00236}{48 \times 7.92} = 2.44 \times 10^{-6} \text{ cm/s}$$

With such an extremely low velocity, the assumption that the fluid inertia may be neglected is certainly justified for this case. It would also be true for any practical case.

It is evident that convection torques could account for the observed fact that a gyro which has been in a fixed position for several days (or even overnight) may take several hours of exercising before performance coefficients are repeatable in a tumble test. It would be interesting to investigate the effects of such density gradients under the following conditions.

- a) A gyro is stored at operating temperature for 30 days with IA up (as in a missile) and then calibrated. Compare the value of D_S obtained in the calibration with the D_S obtained when the gyro is continuously exercised.
- b) Repeat the above test with SA up and compare the value of D_I obtained in the calibration with the D_I obtained when the gyro is continuously exercised.
- c) Compare the change in D_S obtained in (a) with the change in D_I obtained in (b).

If it is determined that convection current effects are significant, then it would be interesting to determine the effects on guidance accuracy in a high g environment of time-varying attitude.

APPENDIX

GLOSSARY OF SYMBOLS

In the general development of the gyro equations in Sections 1, 2, and 3, no dimensional units have been specified and any consistent set may be used. In Sections 4 through 7, commonly used dimensional units have been adopted and it is those dimensional units which are given below. In particular, since angular rates of the gyro case are given in deg/hr rather than in rad/s, it has been necessary to use conversion constants, such as in Eqs. (4-1) and (4-2), which are not required in the earlier equations.

A	= SI symbol for ampere
A_{jk}	= kth vibratory acceleration amplitude (0 to peak) with gyro in Position No. $j - g$
$\bar{a} = \bar{a}_T - \bar{g}$	= applied acceleration vector - g
a_I, a_O, a_S	= components of applied acceleration along I, O, and S axes, respectively - g
$a_{Ijk}, a_{Ojk}, a_{Sjk}$	= components of applied acceleration along I, O, and S axes, respectively, in gyro Position No. j and kth vibration amplitude - g
\bar{a}_T	= total acceleration vector with respect to inertial space - g
a_v	= instantaneous acceleration due to vibration - g
b	= ratio of table rate (relative to earth) to earth rate
c	= damping coefficient
D_F	= fixed restraint (acceleration-insensitive) drift rate - deg/hr
D_I, D_O, D_S	= linear, acceleration-sensitive drift rate coefficients - (deg/hr)/ g
D_{II}, D_{OO}, D_{SS}	= quadratic, acceleration-sensitive drift rate coefficients - (deg/hr)/ g^2
D_{IO}, D_{OS}, D_{IS}	= cross-coupled, acceleration-sensitive drift rate coefficients - (deg/hr)/ g^2
EA	= earth axis (polar axis)

Preceding page blank

F_D	= viscous drag at fluid-gimbal and fluid-gyro case interfaces - dyn/cm ²
G	= acceleration due to gravity - cm/s ²
g	= SI symbol for gram
\underline{g}	= unit of acceleration equal in magnitude to the local (or standard) gravity value
$\bar{\underline{g}}$	= gravity vector (in direction of maximum gravity gradient) - \underline{g}
Π	= angular momentum vector - g · cm ² /s
\bar{H}_g	= angular momentum vector of the gimbal with rotor locked - g · cm ² /s
H_r, \bar{H}_r	= angular momentum and angular momentum vector, respectively, of the gyro rotor (plus associated rotating parts) with respect to the gimbal - g · cm ² /s
H_{rx}, H_{ry}, H_{rz}	= components of \bar{H}_r in the XYZ coordinate system - g · cm ² /s
h	= fluid gap - cm
I, O, S	= orthogonal coordinate axes along IRA, ORA, and SRA, respectively
IA, OA, SA	= true input, output, and spin axes of gimbal, respectively. Not necessarily mutually orthogonal.
IRA, ORA, SRA	= orthogonal input, output, and spin reference axes, respectively, as indicated by markings or mounting surfaces on the gyro case.
$\bar{i}, \bar{j}, \bar{k}$	= unit vectors along I, O, and S axes, respectively
i	= torquing or command-rate current - A
i_{ONk}, i'_{ONk}	= command rate-to-balance current in tumble test Position No. 1, at table angle θ_k , for counterclockwise and clockwise table rates, respectively - A
i_{OSk}, i'_{OSk}	= same as above except gyro is in Position No. 2 - A

i_{jk}	= command rate-to-balance current in vibration test Position No. j at the k th vibration amplitude - A
J_I, J_O, J_S	= moments of inertia of the gimbal about the I, O, and S axes, respectively - $g \cdot cm^2$
J_p	= moment of inertia of a rigid body about a line p passing through the centroid
J_r	= moment of inertia of the gyro rotor (plus associated rotating parts adjusted for speed ratio) about its axis of rotation - $g \cdot cm^2$
J_{uu}, J_{vv}, J_{ww}	= principal moments of inertia of a rigid body
K_e	= elastic restraint coefficient
K_T	= command rate scale factor (deg/hr)/A
k	= 1, 2, 3, ..., n or 0, 1, 2, ..., n
l	= length of gimbal - cm
l_{mn}	= direction cosines of I, O, and S axes with respect to the principal axes
M_I, M_S	= components of applied normalized torque (applied torque/ H_r) about the gimbal I and S axes, respectively
M_C	= component of applied normalized torque about the gimbal O axis plus the normalized viscous drag torque, the normalized elastic restraint torque, and the normalized command torque
M_W	= moment of fluid weight about OA - dyn · cm
M_μ	= total viscous drag moment exerted on the fluid by the gimbal and the gyro case - dyn · cm
$M_{\mu C}$	= viscous drag moment about OA exerted on the gimbal due to fluid flow - dyn · cm
N	= integer
R	= radius - cm
s	= SI symbol for second

T	= period of vibration - s
TA	= table axis
T_I, T_O, T_S	= components of applied torque about I, O, and S axes, respectively
t	= time - s
\bar{t}	= table rate vector relative to earth - deg/hr
U, V, W	= principal axes of inertia
u, v, w	= orthogonal coordinate system fixed to the gyro case
$\bar{u}, \bar{v}, \bar{w}$	= vector components of a variable along the u, v, and w axes, respectively
v_a	= average fluid velocity in gap - cm/s
v_m	= maximum fluid velocity in gap - cm/s
W_{Ijk}, \bar{W}_{Ijk}	= instantaneous and average values, respectively, of the command rate-to-balance in vibration test Position No. j and at the kth vibration amplitude - deg/hr
W_{ONk}, W_{OSk}	= weighted drift rates in tumble test at table angle θ_k in Positions No. 1 and No. 2, respectively - deg/hr
X, Y, Z	= orthogonal coordinate system fixed to gimbal
x, y, z	= earth-fixed orthogonal coordinate system
$\bar{x}, \bar{y}, \bar{z}$	= vector components of a variable along the x, y, and z axes, respectively
α	= angle that an east-west line makes with a plane parallel to TA and EA - rad
β_1, β_2	= angle that an east-west line makes with a plane parallel to TA and ORA at table angle $\theta_k = 0$ deg in tumble test Positions No. 1 and No. 2, respectively - rad
$\delta_{ONT}, \delta_{OST}$	= angle that ORA makes with TA in tumble test Positions No. 1 and No. 2, respectively - rad
δ_{TE}	= angle that TA makes with EA - rad
ζ_I	= $\zeta_x - \zeta_{rx}$

δ_O	= δ_Y
ϵ_{rx}	= angle that SA' makes with the Z axis, where SA' is the projection of SA on the YZ plane - rad
$\epsilon_x, \epsilon_y, \epsilon_z$	= small Euler angles required to rotate the XYZ coordinate system into coincidence with the IOS coordinate system when $\varphi_O = 0$ - rad
θ	= table angle measured from east-west line in direction of earth's rotation - deg
θ	= angle about OA from IA to any point in fluid gap - rad
θ_k	= $k\theta_n$, where $k = 1, 2, 3, \dots, n$ - deg
θ_n	= $360^\circ/n$, where n is an integer - deg
$\theta_u, \theta_v, \theta_w$	= small Euler angles required to rotate the UVW coordinate system into coincidence with the IOS coordinate system - rad
λ	= astronomic latitude (positive in northern hemisphere) - deg
μ	= viscosity - poise = $\text{dyn} \cdot \text{s}/\text{cm}^2$
ρ_0	= fluid density at $\theta = 0$ deg - g/cm^3
ρ_θ	= fluid density at angle θ - g/cm^3
$\Delta\rho$	= $\rho_{90} - \rho_{270}$ - g/cm^3
φ_O	= angular displacement of the gimbal from its electrical null position - rad
ω	= circular frequency - rad/s
ω_E	= earth rate - deg/hr
$\omega_I, \omega_O, \omega_S$	= angular velocity components of the gyro case relative to inertial space about the I, O, and S axes, respectively - deg/hr
$\omega_{IE}, \omega_{OE}, \omega_{SE}$	= components of earth rate about the I, O, and S axes, respectively - deg/hr
ω_r	= angular velocity of the rotor relative to the gimbal - rad/s